Annals of Botany **127**: 749–764, 2021
doi: 10.1093/aob/mcab033, available online at www.academic.oup.com/aob

ANNALS OF BOTANY
Founded 1887

Gene expression underlying floral epidermal specialization in *Aristolochia fimbriata* (Aristolochiaceae)

Harold Suárez-Baron[1], Juan F. Alzate[2], Favio González[3], Soraya Pelaz[4,5,*], Barbara A. Ambrose[6] and Natalia Pabón-Mora[1,*]

[1]Instituto de Biología, Universidad de Antioquia, Medellín, Colombia, [2]Centro Nacional de Secuenciación Genómica (CNSG), Sede de Investigación Universitaria, Facultad de Medicina, Universidad de Antioquia, Medellín, Colombia, [3]Universidad Nacional de Colombia, Facultad de Ciencias, Instituto de Ciencias Naturales, Bogotá, Colombia, [4]Centre for Research in Agricultural Genomics, CSIC-IRTA-UAB-UB, Campus UAB, Bellaterra, Barcelona, Spain, [5]ICREA (Institució Catalana de Recerca i Estudis Avançats), Barcelona, Spain and [6]The New York Botanical Garden, Bronx, NY, USA
**For correspondence. E-mail lucia.pabon@udea.edu.co*

Received: 16 October 2020 Returned for revision: 7 February 2021 Editorial decision: 19 February 2021 Accepted: 22 February 2021
Electronically published: 25 February 2021

• **Background and Aims** The epidermis constitutes the outermost tissue of the plant body. Although it plays major structural, physiological and ecological roles in embryophytes, the molecular mechanisms controlling epidermal cell fate, differentiation and trichome development have been scarcely studied across angiosperms, and remain almost unexplored in floral organs.
• **Methods** In this study, we assess the spatio-temporal expression patterns of *GL2*, *GL3*, *TTG1*, *TRY*, *MYB5*, *MYB6*, *HDG2*, *MYB106*-like, *WIN1* and *RAV1*-like homologues in the magnoliid *Aristolochia fimbriata* (Aristolochiaceae) by using comparative RNA-sequencing and *in situ* hybridization assays.
• **Key Results** Genes involved in *Aristolochia fimbriata* trichome development vary depending on the organ where they are formed. Stem, leaf and pedicel trichomes recruit most of the transcription factors (TFs) described above. Conversely, floral trichomes only use a small subset of genes including *AfimGL2*, *AfimRAV1*-like, *AfimWIN1*, *AfimMYB106*-like and *AfimHDG2*. The remaining TFs, *AfimTTG1*, *AfimGL3*, *AfimTRY*, *AfimMYB5* and *AfimMYB6*, are restricted to the abaxial (outer) and the adaxial (inner) pavement epidermal cells.
• **Conclusions** We re-evaluate the core genetic network shaping trichome fate in flowers of an early-divergent angiosperm lineage and show a morphologically diverse output with a simpler genetic mechanism in place when compared to the models *Arabidopsis thaliana* and *Cucumis sativus*. In turn, our results strongly suggest that the canonical trichome gene expression appears to be more conserved in vegetative than in floral tissues across angiosperms.

Key words: *Aristolochia*, epidermis development, multicellular trichomes, perianth, petaloid sepals, Piperales.

INTRODUCTION

The epidermis is the continuous surface tissue in embryophytes, and it is fundamental for plant integrity. Specialized epidermal cells such as stomatal guard cells and trichomes are essential for the structural integrity and physiology of plants, and for their interplay with the environment (Javelle *et al.*, 2011). Trichomes are highly differentiated epidermal cells present mainly on the exposed aerial plant organs, thus acting as micromorphological structures often correlated to environmental conditions (Pattanaik *et al.*, 2014; Ioannidi *et al.*, 2016). The morphology, function, shape, size, location and density of trichomes are species-specific, thus being exceedingly diverse and specialized (Netolitzky, 1932; Wagner *et al.*, 2004).

Trichome functions depend primarily on the organs from which they develop. For instance, trichomes in leaves can regulate temperature, reduce water loss, increase light reflectance, prevent abrasion, and protect inner tissues from UV radiation as well as from insect and pathogen attack (Levin, 1973; Wagner, 1991; Karabourniotis *et al.*, 1992; Werker, 2000; Wagner *et al.*, 2004; Pattanaik *et al.*, 2014). Trichomes in flowers might play structural roles during flower synorganization (El Ottra *et al.*, 2013; Tan *et al.*, 2016), promote toxin synthesis, and act as active mechano-sensory switches and wave detectors during herbivory (Zhou *et al.*, 2016; Liu *et al.*, 2017). Floral trichomes also play key mechanical and biochemical functions in various pollination syndromes (Young *et al.*, 1984; Cropper and Calder, 1990; Cocucci, 1991; Hu *et al.*, 2008; Martins *et al.*, 2013; Boff *et al.*, 2015; Płachno *et al.*, 2018, 2019; Stpiczyńska *et al.*, 2018). For instance, trichomes inside the *Aristolochia* (Aristolochiaceae) perianth are specialized either as mechanical structures to temporarily trap insects, or as secretory trichomes to feed them (Dafni, 1984; Oelschlägel *et al.*, 2009; Pabón-Mora *et al.*, 2015; Erbar *et al.*, 2016; Suárez-Baron *et al.*, 2019).

The flowers of *Aristolochia* are considered 'trap-flowers' with a complex architecture and pollination mechanism (Oelschlägel *et al.*, 2009; Pabón-Mora *et al.*, 2015; Erbar *et al.* 2016). The perianth is monosymmetric and formed by three fused sepals that variously curve forming a basal, inflated

portion called the *utricle*, a narrow portion called the *tube*, and a distal, expanded, laminar coloured portion called the *limb*, which serves as the platform for visiting insects (Fig. 1) (González and Stevenson, 2000). Their pollinators – mainly flies – land on the limb, probably attracted by colour and scent, then pass through the tube and reach the utricle. The perianth tube is covered by downward-pointing multicellular trichomes that trap the flies in the utricle for a few days. Here flies release pollen grains in the mature stigmas. After ovule fertilization, stamens mature and deposit new pollen on the flies, which after perianth withering and loss of trichome turgor, escape loaded with fresh pollen (Oelschlägel *et al.*, 2009; Pabón-Mora *et al.*, 2015). For adequate functioning of such a floral trap, the adaxial (inner) epidermis has different specialized trichomes in each of the floral portions. The adaxial epidermis of the utricle is carpeted with multicellular, filamentous, secretory trichomes interspersed by osmophores. Conversely, the adaxial epidermis of the limb and the tube is covered by multicellular hooked and conical trichomes, respectively, both performing mechanical roles (Fig. 1).

Trichome differentiation responds to both external signals and endogenous developmental programmes; thus, it is the result of a tightly regulated interplay between positional cues, intercellular communication and morphogenesis that results in cell fate specification (Szymanski *et al.*, 2000; Hulskamp, 2004). The core genetic mechanisms underlying trichome identity and development have been identified in model flowering plants (Larkin *et al.*, 1996, 1997; Glover *et al.*, 1998; Glover, 2000; Schwab *et al.*, 2000; Szymanski *et al.*, 2000; Kärkkäinen and Ågren, 2002; Schnittger and Hülskamp, 2002, 2005; Machado *et al.*, 2009; Zhao *et al.*, 2015*b*). In *Arabidopsis*, the development of unicellular trichomes is the result of an activator–inhibitor complex. Mutant plants of positive regulators for trichome development have fewer or no trichomes, compared to the wild type. (Digiuni *et al.*, 2008). Trichome activators include the *R2R3 MYB* transcription factor (TF), *GLABRA1* (*GL1*), the redundant basic helix–loop–helix (bHLHs) factors *GLABRA3* (*GL3*) and *ENHANCER OF GLABRA3* (*EGL3*), and the WD40-repeat protein *TRANSPARENT TESTA GLABRA1* (*TTG1*) (Oppenheimer *et al.*, 1991; Galway *et al.*, 1994; Walker *et al.*, 1999; Payne *et al.*, 2000; Zhang *et al.*, 2003; Bernhardt *et al.*, 2003, 2005; Kirik *et al.*, 2005; Simon *et al.*, 2013). Yeast two-hybrid protein interaction assays indicate that GL3 physically interacts with GL1 and TTG1; in turn this MYB–bHLH–WD40 (MBW) activation complex directly controls trichome formation (Rerie *et al.*, 1994; Payne *et al.*, 2000; Schiefelbein, 2003; Pesch and Hülskamp, 2004; Serna and Martin, 2006). The downstream target gene of the MBW complex is the homeodomain-leucine zipper *GLABRA2* (*GL2*), which initiates trichome differentiation (Rerie *et al.*, 1994; Cristina *et al.*, 1996; Masucci *et al.*, 1996; Hülskamp, 2004; Pesch and Hülskamp, 2009). This complex is inhibited when the R2R3 MYB protein is replaced by an R3 MYB protein (Payne *et al.*, 2000). Thus, negative regulators for trichome development include several small single-repeat R3 MYB TFs, such as TRIPTYCHON (TRY), CAPRICE (CPC), and

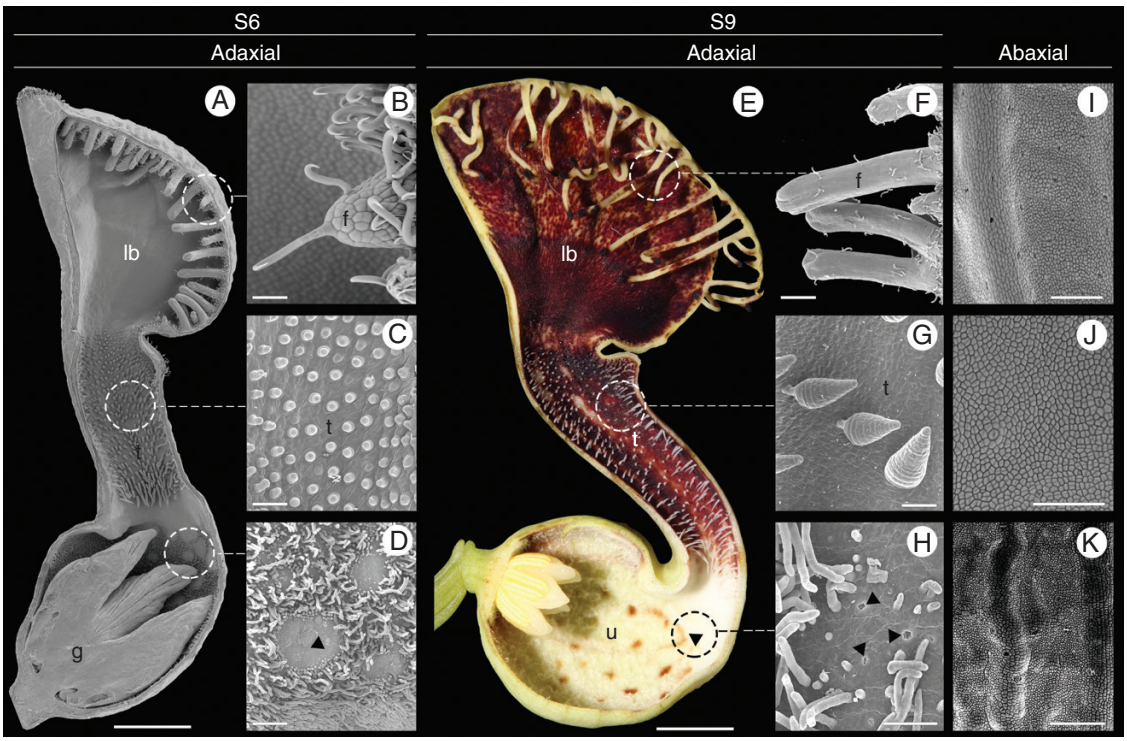

FIG. 1. *Aristolochia fimbriata*, flower morphology and epidermal differentiation of the perianth. (A and E) Sagittal section through flowers at S6 (A) and S9 (E) stages. (B and F) Detail of fimbriae at S6 (B) and S9 (F); note hooked trichomes. (C and G) Secretory multicellular, conical trichomes on the adaxial epidermis of the tube at S6 (C) and S9 (G). (D and H) Detail of the utricle adaxial epidermis with osmophores surrounded by secretory, filamentous multicellular trichomes. (I–K) Detail of the abaxial epidermis of the limb (I), tube (J) and utricle (K), with scattered stomata. Arrowheads: osmophores; f, fimbriae; g, gynostemium; lb, limb; t, tube; u, utricle. Scale bars: 1 mm (A); 100 µm (B–D, I, K); 5 mm (E); 50 µm (F–H, J).

ENHANCER OF TRY AND CPC1 and 2 (ETC1 and ETC2) (Hülskamp *et al.*, 1994; Wada *et al.*, 1997, 2002; Szymanski and Marks, 1998; Schnittger *et al.*, 1999; Schellmann *et al.*, 2002; Esch *et al.*, 2004; Kirik *et al.*, 2004*a*, *b*) (Fig. 2A). Furthermore, additional regulatory genes have been reported such as *MYB5*, having a redundant role with the *R2R3 MYB* gene *TRANSPARENT TESTA GLABRA2* (*TTG2*) in the control of trichome development, branching and tannin production (González *et al.*, 2009; Li *et al.*, 2009; Marks *et al.*, 2009). Also, *MYB106* controls trichome branching in *Arabidopsis* (Folkers *et al.*, 1997; Stracke *et al.*, 2001; Jakoby *et al.*, 2008), epidermal conical cell development in flowers of *Antirrhinum majus* and *Nicotiana tabacum* (Noda *et al.*, 1994; Baumann *et al.*, 2007; Jaffé *et al.*, 2007), and multicellular trichomes in *Cucumis sativus* (Zhao *et al.*, 2015*b*; Yang *et al.*, 2018). In addition, the *HOMEODOMAIN GLABROUS 2* (*HDG2*) has been reported as a key epidermal component promoting stomatal differentiation and trichome cell wall development in *Arabidopsis* (Marks *et al.*, 2009; Peterson *et al.*, 2013). Finally, *RAV* genes have been associated with the regulation of trichome initiation in *Arabidopsis* (Matías-Hernández *et al.*, 2016) and *Cucumis sativus* (Zhao *et al.*, 2015*a*).

Unicellular trichomes have been, by far, more studied than multicellular trichomes. However, scattered data on the genetic

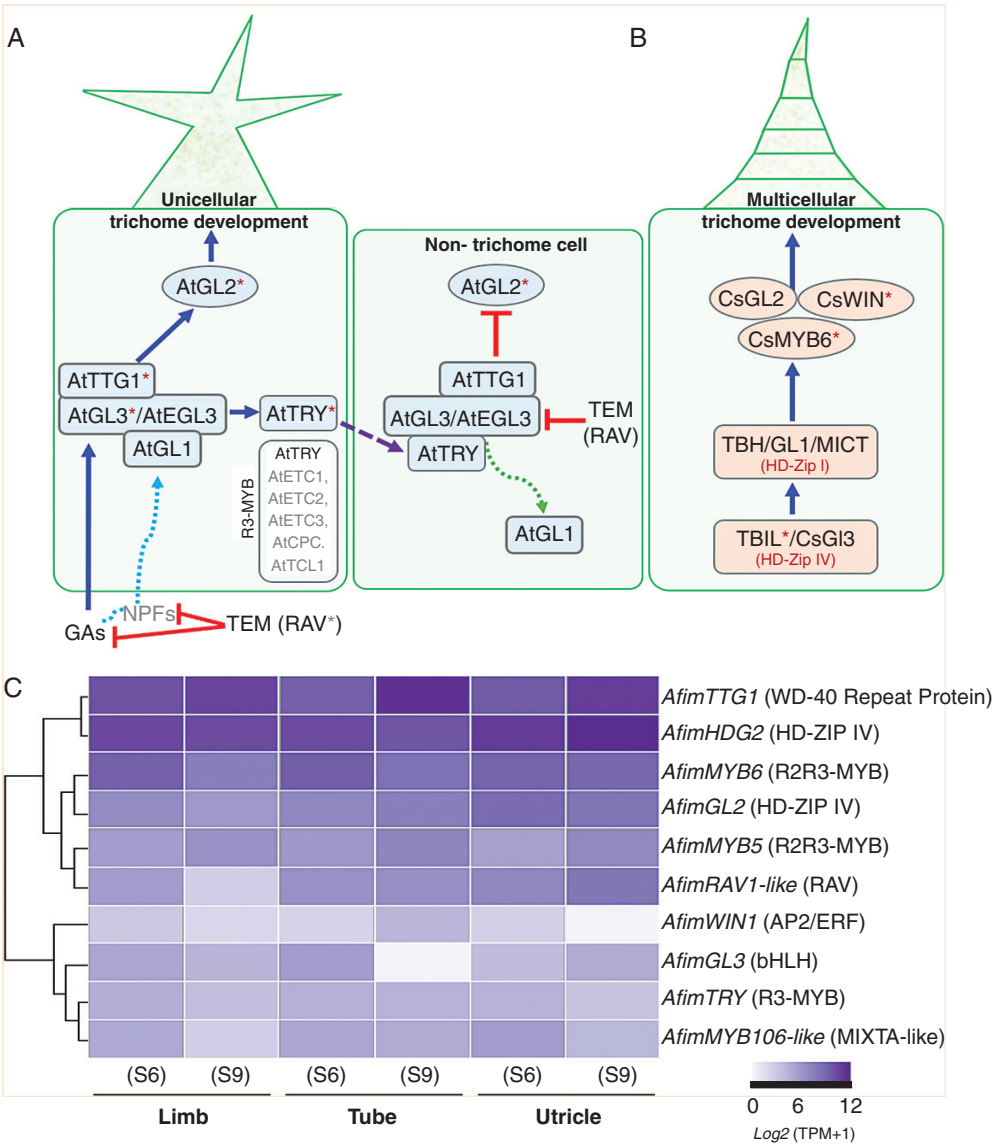

FIG. 2. Canonical signalling pathways for unicellular and multicellular trichome development and comparative expression in *Aristolochia fimbriata*. (A) Schematic model of Arabidopsis trichome differentiation and surrounding pavement cell fate specification (modified from Zhao *et al.*, 2008; Matías-Hernández *et al.*, 2016). The activation complex is formed by GL1, TTG1 and GL3/EGL3 proteins. This complex activates transcription of GL2 to promote trichome formation while an *R3-MYB* repressor protein (TRY) moves to the neighbouring cells to repress trichome formation. *R3-MYB* members including TRY, CPC, ETC1, 2, 3 and TCL1 repress trichome initiation. RAV genes repress trichome initiation via gibberellins. (B) Proposed model for multicellular trichome patterning in *Cucumis sativus* (modified from Liu *et al.*, 2016). Asterisks indicate the homologues evaluated in this study. (C) Heatmap displaying the expression of the ten candidate genes selected from the two models above. The relative abundance of transcript per million (TPM) values is shown for *AfimGL2*, *AfimGL3*, *AfimHDG2*, *AfimMYB5*, *AfimMYB6*, *AfimMYB106*-like, *AfimRAV1*-like, *AfimTRY*, *AfimTTG1* and *AfimWIN1* in the three perianth portions at S6 and S9.

bases for the latter have been gathered in a few core eudicot model taxa, suggesting that the same MBW complex is in place (Yang *et al.*, 2015). In *Nicotiana tabacum*, homologues of *MIXTA* (also a *MYB* homologue) are able to induce multicellular trichome formation (Payne *et al.*, 1999; Perez-Rodriguez *et al.*, 2005). In *Cucumis sativus*, *CsGL2*, *CsMYB6* and *CsWIN1* are directly involved in multicellular trichome development (Chen *et al.*, 2014; Li *et al.*, 2015; Pan *et al.*, 2015; Zhao *et al.*, 2015*a*, *b*; Cui *et al.*, 2016; Liu *et al.*, 2016; Wang *et al.*, 2016; Yang *et al.*, 2018).

The genetic mechanisms underlying the formation of floral trichomes in non-model species outside rosids and asterids are poorly understood. Here we aim to assess the spatio-temporal expression patterns of the candidate trichome-development homologues (*GL2*, *GL3*, *TTG1*, *TRY*, *MYB5*, *MYB6*, *HDG2*, *MYB106*-like, *WIN1* and *RAV1*-like) in *Aristolochia fimbriata*, by combining different state-of-the-art methodologies, including comparative transcriptomics [RNA-sequencing (RNA-seq)] and *in situ* hybridization assays. We present a detailed expression profile of key regulatory genes that participate in the epidermal differentiation of the *A. fimbriata* perianth. Thus, our goal is to test whether candidate genes for trichome development and epidermal elaboration identified in model species are involved in the initiation and development of specialized, multicellular trichomes in vegetative and floral organs of *Aristolochia.*

MATERIALS AND METHODS

Transcriptome analysis

De novo transcriptomes from *Aristolochia fimbriata* were generated. Each transcriptome was obtained from three independent biological replicates of the three dissected portions of the sepal-derived perianth (utricle, tube and limb), at two floral developmental stages, namely S6 and S9 (stages follow Pabón-Mora *et al.*, 2015; Fig. 1). Total RNA from all dissected perianth portions at both stages (Fig. 1) was extracted using TRIZOL reagent (Invitrogen). The RNA-seq experiment was conducted using the Truseq stranded mRNA library construction kit (Illumina) and sequenced on a NovaSeq 6000 system reading 100-bp, paired-end reads. Read cleaning was performed with a homebrew program with a quality threshold of Q30 at both ends and only keeping those longer that 70 bases after trimming. Contig assembly was computed using the Trinity package following default settings. Transcriptome assembly was performed for each perianth portion, in both developmental stages (Supplementary Data Table S1). In addition, a combined global transcriptome from all experiments was assembled as a reference with the following metrics: total assembled bases: 85 608 833 bp; total number of contigs (> 101 bp): 118 941; average contig length: 719 bp; contig N50: 14 432 sequences ≥ 1823 bp; contig N75: 31 828 sequences ≥ 746 bp; contig GC%: 42.71%.

Gene homologue searches and phylogenetic analyses

The sequences of all candidate genes involved in epidermis and trichome development were retrieved from the global *Aristolochia fimbriata* transcriptome using *tblastx*. The queries included the canonical target genes of *Arabidopsis GL2*, *GL3*, *TTG1*, *TRY*, *MYB5*, *MYB6*, *HDG2*, *WIN1*, *RAV1*-like and *MYB106/NOK*, as well as the *MIXTA* gene from *Antirrhinum majus.* All resulting contigs were confirmed by performing reciprocal searches in GenBank (https://blast.ncbi.nlm.nih.gov/Blast.cgi), and manually curated to identify the open reading frame, coding DNA sequence and untranslated regions (UTRs). Isolated sequences in this study correspond to GenBank accession numbers: MT365930–MT365939.

To assess homology for all genes isolated, we performed comprehensive phylogenetic analyses for all gene lineages. These analyses were based on an expanded sampling of the *GL2*, *GL3*, *TTG1*, *TRY*, *MYB5*, *MYB6*, *HDG2*, *MYB106*-like, *WIN1* and *RAV1*-like homologues obtained from eudicots, monocots and magnoliids, using the following repositories: the genome database Phytozome (https://phytozome.jgi.doe.gov/pz/portal.html), GenBank (NCBI) nucleotide database (https://www.ncbi.nlm.nih.gov/nucleotide/) and the transcriptome database OneKP (https://db.cngb.org/blast/). Sequences were compiled using BioEdit (http://www.mbio.ncsu.edu/bioedit/bioedit.html). Nucleotide sequences were then aligned using the online version of MAFFT (https://mafft.cbrc.jp/alignment/server/) (Katoh *et al.*, 2002), with a gap open penalty of 3.0, offset value of 1.0 and all other settings as default. Then, alignments were refined by hand using BioEdit considering the representative conserved domains for each of the targeted gene families. Maximum likelihood (ML) phylogenetic analyses using the full nucleotide sequences for each gene were performed with RaxML-HPC2 BlackBox (https://www.phylo.org/) (Stamatakis *et al.*, 2008), through the CIPRES Science Gateway (Miller *et al.*, 2010). Bootstrapping was performed according to the default criteria in RaxML where the bootstrapping stopped after 200–600 replicates when the criteria were met. Trees were observed and edited using FigTree v.1.4.4. (http://tree.bio.ed.ac.uk/software/figtree/) (Rambaut, 2014). Homologues from *Amborella trichopoda* were used as the outgroups in all phylogenetic analyses (Supplementary Data Table S2).

Mapping, gene annotation and expression by RNA-seq

To estimate the relative abundance of the assembled contigs, cleaned reads were mapped against the *de novo* assembled dataset implementing the algorithm Kallisto v.0.46.0 with default settings (https://pachterlab.github.io/kallisto/). Kallisto quantifies transcript expression normalizing the relative abundance of each contig/transcript using transcript per million (TPM) metrics (Bray *et al.*, 2016) (Supplementary Data Table S3). The relative abundance of *GL2*, *GL3*, *TTG1*, *TRY*, *MYB5*, *MYB6*, *HDG2*, *MYB106*-like, *WIN1* and *RAV1*-like transcripts was used to identify their expression level in each portion of the *Aristolochia fimbriata* perianth. This expression was calculated for the six generated transcriptomes corresponding to the utricle, the tube, and the limb at two different developmental stages (S6 and S9). Expression data from each sample were used to construct the heatmaps using the R package *pheatmap* (https://cran.r-project.org/web/packages/pheatmap/index.html).

Material collection and expression analyses by in situ hybridization assays

Flowers of *Aristolochia fimbriata* at different developmental stages were collected from plants growing in the Nolen glasshouses at the New York Botanical Garden (NYBG) or at the Universidad de Antioquia (UdeA), and fixed under vacuum in freshly prepared, cold formaldehyde–acetic acid–ethanol (FAA solution: 50% ethanol, 37% formaldehyde and 5% glacial acetic acid). After a 4-h incubation, samples were dehydrated in an ethanol series and then transferred to fresh Paraplast X-tra tissue embedding medium (Fisher, Waltham, MA, USA) in a Leica TP1020 automatic tissue processor and stored at 4 °C until use. Samples were prepared and sectioned at 10 µm on a Microm HM3555 rotary microtome. DNA templates for RNA probe synthesis were obtained by PCR amplification of 300–550-bp fragments. To ensure specificity, the probe templates were designed to amplify the 3′ UTR sequences from each evaluated gene (Supplementary Data Table S4). Fragments were cleaned using the QIAquick PCR purification Kit (Qiagen, Valencia, CA, USA). Digoxigenin-labelled RNA probes were prepared using T7 polymerase (Roche, Switzerland), murine RNAse inhibitor (New England Biolabs, Ipswich, MA, USA), and RNA labelling mix (Roche) according to each manufacturer's protocols. RNA *in situ* hybridization was performed according to Ambrose *et al.* (2000) and Ferrándiz *et al.* (2000), optimized to hybridize overnight at 55 °C. Probe concentration was identical for all the experiments, including the sense control hybridizations. *In situ* hybridized sections were subsequently dehydrated and permanently mounted in Permount (Fisher). All sections were digitally photographed using a Zeiss Axioplan microscope equipped with a Nikon DXM1200C digital camera.

RESULTS

Identification of epidermis- and trichome-related genes in Aristolochia fimbriata

Targeted blast searches on the global transcriptome of *Aristolochia fimbriata* followed by phylogenetic analyses (Supplementary Data Figs S1–S10) allowed us to identify single-copy gene homologues for *GL2* (named *AfimGL2*), *GL3* (*AfimGL3*), *HDG2* (*AfimHDG2*), *MYB5* (*AfimMYB5*), *MYB6* (*AfimMYB6*), *MYB106*-like (*AfimMYB106*-like), *RAV1*-like (*AfimRAV1*-like), *TRY* (*AfimTRY*), *TTG1* (*AfimTTG1*) and *WIN1* (*AfimWIN1*). We did not find homologues of *GL1* or *EGL3* genes.

Comparative gene expression from RNA-seq analyses

Comparative expression levels of the ten candidate genes were tested in the utricle, tube and limb at developmental stages S6 and S9 (Fig. 1). The analyses revealed active expression of a subset of the targeted genes, namely the TFs *AfimTTG1*, *AfimHDG2*, *AfimMYB6*, *AfimGL2*, *AfimMYB5* and *AfimRAV1*-like (Fig. 2C). Most genes that were differentially expressed in the tube and the utricle tended to increase in expression from S6 to S9. This was the case for *AfimTTG1* and *AfimMYB5* in the limb, tube and utricle. Those with the opposite trend (reduced levels at S9 when compared to S6) include *AfimRAV1*-like in the limb, and *AfimMYB6* in the limb and tube. Conversely, *AfimWIN1*, *AfimGL3*, *AfimTRY* and *AfimMYB106*-like had lower expression levels in all floral portions during the two developmental stages. From the core *Arabidopsis* trichome-activating complex (GL1–GL3/EGL3–TTG1), only *AfimTTG1* had significant expression levels in the limb, tube and utricle. In contrast, *AfimWIN1* had a homogeneous low expression across developmental stages in the limb, tube and utricle, with increased expression at S6. *AfimGL2*, which is the putative downstream target of this complex, was expressed in all perianth portions, with significant expression levels in both the tube and the utricle. The single-repeat MYB *AfimTRY*, which in *Arabidopsis* negatively regulates the trichome-activating complex, presented a homogeneous lower expression. Similar patterns were found for *AfimMYB106*-like which is a positive regulator of trichome development in *Cucumis sativus* (Fig. 2C).

Detailed expression by in situ hybridization

With the aim of identifying putative trichome patterning candidate genes, we investigated the spatial and temporal expression patterns of ten TFs. We used RNA *in situ* hybridization assays on transverse and longitudinal sections of the *Aristolochia fimbriata* flower throughout developmental stages S1–S6 (stages following Pabón-Mora *et al.*, 2015) and the leaves. These experiments provided information on the mRNA spatio-temporal expression patterns of the candidate genes. mRNA localization is probably correlated with, but are not necessarily equivalent to, the protein, as the latter can be narrowed by degradation or broadened by translocation between cells. Descriptions hereafter focus on expression changes between the adaxial (inner) and the abaxial (outer) perianth epidermis in flowers at S5–S6. Particular attention was given to expression in the floral trichomes.

Most highly expressed TFs in both the adaxial and the abaxial floral epidermis include AfimGL2, AfimRAV1-like, AfimWIN1 and AfimMYB106-like homologues

Expression of *AfimGL2*, *AfimWIN1* and *AfimRAV1*-like genes was detected in the shoot apical meristem, as well as in the young leaves and in the perianth at S1–S2 (Supplementary Data Fig. S11), while expression of *AfimMYB106*-like at these early stages was weak (Fig. S11). Expression of these four TFs during S3–S4 (perianth and ovary differentiation) was found throughout the perianth, in the developing gynostemium and in the ovary (Fig. S11). During S6 all four TFs were expressed between the midvein and the adaxial epidermis of the perianth (Figs 3A–6A), where more subepidermal cell layers showed expression in the limb and tube (~12) compared to the utricle (~4–6). Expression of these four TFs was also evident in the fimbriae, which are vascularized limb extensions with distal osmophores probably involved in attracting

pollinators (González and Pabón-Mora, 2015) (Fig. 1B, F). Furthermore, *AfimMYB106* was expressed in the marginal portion of the limb and *AfimWIN1* and *AfimRAV1*-like were also detected in the hooked trichomes scattered in the limb (Figs 3C, D, 4C, D, 5C, D and 6C, D). *AfimGL2*, *AfimMYB106*-like, *AfimRAV1*-like and *AfimWIN1* were also detected in the multicellular, conical trichomes formed on the adaxial epidermis of the tube (Figs 3F, G, 4F, G, 5F, G and 6F, G), and the secretory, multicellular, filamentous trichomes inside the utricle (Figs 3I, J, 4I, J, 5I, J and 6I, J). Also, flowers at S6 showed expression of *AfimMYB106*-like and *AfimWIN1* in the abaxial epidermis of the utricle, tube and limb (Figs 4A–J and 5A–J). Conversely, *AfimGL2* was weakly expressed and *AfimRAV1*-like was undetected in the abaxial perianth epidermis (Figs 2A–J and 6A–J). Interestingly, only *AfimMYB106*-like and *AfimWIN1* were clearly expressed in the perianth vascular bundles (Figs 4A–J and 5A–J). *AfimGL2*, *AfimMYB106*-like, *AfimWIN1* and *AfimRAV1*-like also presented similar expression patterns in the floral pedicel, specifically in the epidermis and the hooked trichomes (Figs 3L, M, 4L, M, 5L, M and 6L, M). Expression in leaves was detected only for *AfimGL2* and *AfimRAV1*-like (Figs 3K and 6K), but not for *AfimWIN1* or *AfimMYB106*-like (Figs 4K and 5K). Control sense probes for *AfimGL2*, *AfimRAV1*-like, *AfimWIN1* and *AfimMYB106*-like genes showed no signal (Fig. S12).

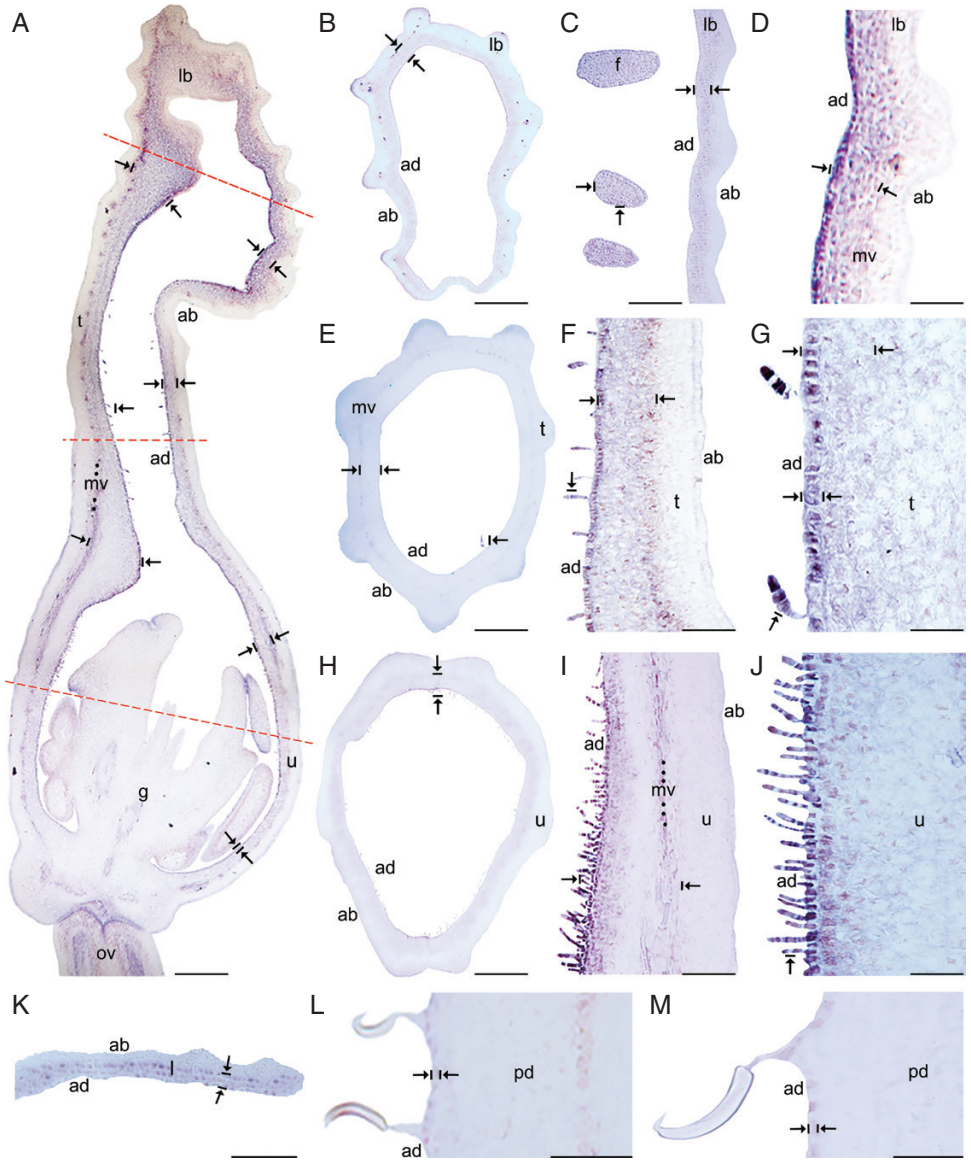

Fig. 3. *In situ* hybridization of *AfimGL2*. (A) Sagittal section of the *Aristolochia fimbriata* flower at S6; note low expression in the abaxial epidermis with respect to the adaxial epidermis. (B–D) Transverse (B) and longitudinal (C, D) sections of the limb at low (B), mid- (C) and high (D) magnification. (E–G) Transverse (E) and longitudinal (F, G) sections of the tube at low (E), mid- (F) and high (G) magnification. (H–J) Transverse (H) and longitudinal (I, J) sections of the utricle at low (H), mid- (I) and high (J) magnification. (K) Transverse section of the leaf. (L–M) Longitudinal section of the floral pedicel and detail of its hooked trichomes (M) adaxial (ad) of the pedicel here and in Figs 4–8 is given in reference to the shoot axis. Arrow/bar signs point to tissue with positive expression; ab, abaxial epidermis; ad, adaxial epidermis; fi, fimbriae; g, gynostemium; l, leaf; lb, limb; mv, midvein; ov, ovary; pd, pedicel; t, tube; u, utricle. Scale bars: 100 µm (A, B, E, H); 150 µm (C, F, I); 200 µm (D, G, J); 60 µm (K–M).

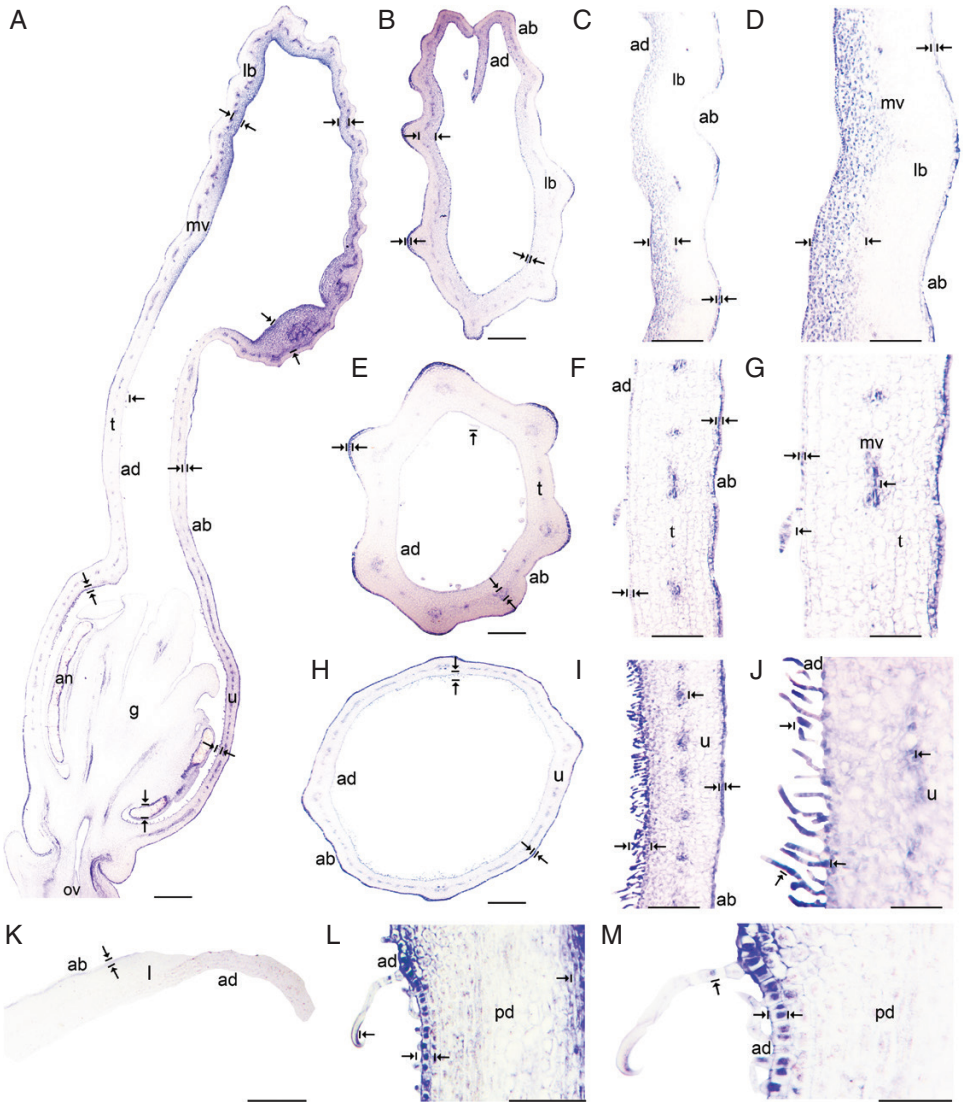

FIG. 4. *In situ* hybridization of *AfimMYB106*-like gene. (A) Sagittal section of the *Aristolochia fimbriata* flower at S6; note strong expression in the adaxial limb mesophyll and the abaxial epidermis. (B–D) Transverse (B) and longitudinal (C, D) sections of the limb at low (B), mid- (C) and high (D) magnification. (E–G) Transverse (E) and longitudinal (F, G) sections of the tube at low (E), mid- (F) and high (G) magnification. (H–J) Transverse (H) and longitudinal (I–J) sections of the utricle at low (H), mid- (I) and high (J) magnification. (K) Transverse section of the leaf. (L–M) Longitudinal section of the floral pedicel and detail of its hooked trichomes (M). Arrow/bar signs point to tissue with positive expression; ab, abaxial epidermis; ad, adaxial epidermis; an, anther; fi, fimbriae; g, gynostemium; l, leaf; lb, limb; mv, midvein; ov, ovary; pd, pedicel; t, tube; u, utricle. Scale bars: 100 µm (A, B, E, H); 150 µm (C, F, I); 200 µm (D, G, J); 60 µm (K–M).

TFs preferentially restricted to the abaxial floral epidermis include AfimHDG2, AfimTTG1, AfimGL3, AfimTRY, AfimMYB5 and AfimMYB6

AfimHDG2 was weakly detected in the perianth at S4 (Supplementary Data Fig. S11). During S6 (Fig. 7A), expression of *AfimHDG2* was detected in both the abaxial and the adaxial perianth epidermis. However, expression was always higher in the abaxial epidermis, when compared to the adaxial counterpart. Similar expression levels were detected in the limb (Fig. 7B, C), tube (Fig. 7F, G) and utricle (Fig. 7I, J). Expression of *AfimHDG2* beyond the perianth was found in the hooked trichomes and the epidermis of the pedicel (Fig. 7L, M). Finally, no expression was detected in the young leaves (Fig. 7K). Control sense probes for *AfimHDG2* resulted in no signal (Fig. S12).

The TFs *AfimGL3*, *AfimMYB5*, *AfimMYB6*, *AfimTRY* and *AfimTTG1* were weakly expressed at S1–S4 in the perianth, anther primordia and ovary (Supplementary Data Fig. S11). During S6, *AfimGL3*, *AfimMYB5*, *AfimMYB6*, *AfimTRY* and *AfimTTG1* homologues presented a similar expression pattern restricted to the abaxial epidermis of the perianth (Fig. 8; Figs S13–S16). Expression in the abaxial epidermis was detected in the limb (Fig. 8A, C–D; Figs S13–S16A–B, D), tube (Fig. 8A, E-G; Figs S13–S16A, E–G) and utricle (Fig. 8A, H–J; Figs S13–S16A, H–J). At S6, none of these five TFs was detected in the multicellular, conical trichomes inside the tube or the secretory, multicellular, filamentous trichomes inside the utricle (Fig. 8F, G, I, J; Figs S13–S16F, G, I, J) or in the vascular bundles of the perianth (Fig. 8; Figs S13–S16). However, expression of *AfimTTG1*, *AfimGL3*, *AfimTRY*,

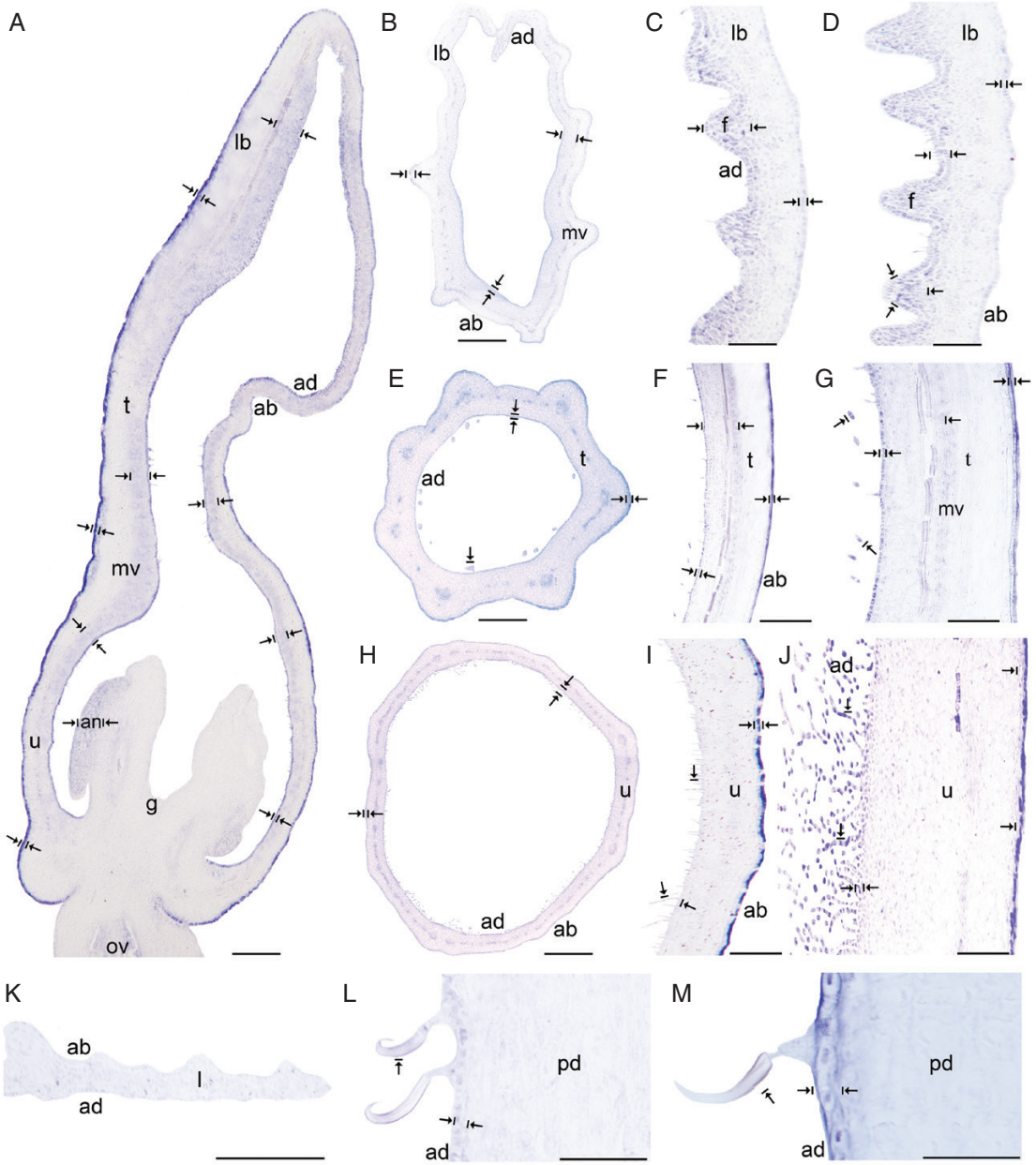

FIG. 5. *In situ* hybridization of *AfimWIN1*. (A) Sagittal section of the *Aristolochia fimbriata* flower at S6; note higher expression in the adaxial perianth mesophyll, the fimbriae and the abaxial epidermis of the perianth. (B–D) Transverse (B) and longitudinal (C, D) sections of the limb at low (B), mid- (C) and high (D) magnification. (E–G) Transverse (E) and longitudinal (F, G) sections of the tube at low (E), mid- (F) and high (G) magnification. (H–J) Transverse (H) and longitudinal (I–J) sections of the utricle at low (H), mid- (I) and high (J) magnification. (K) Transverse section of the leaf. (L–M) Longitudinal section of the floral pedicel (L) and detail of its hooked trichomes (M). Arrow/bar signs point to tissue with positive expression; ab, abaxial epidermis; ad, adaxial epidermis; an, anther; fi, fimbriae; g, gynostemium; l, leaf; lb, limb; mv, midvein; ov, ovary; pd, pedicel; t, tube; u, utricle. Scale bars: 100 µm (A, B, E, H); 150 µm (C, F, I); 200 µm (D, G, J); 60 µm (K–M).

AfimMYB5 and *AfimMYB6* was detected in the epidermis and the subepidermal layer of the floral pedicel, and in the three-celled hooked trichomes (Fig. 8L–M; Figs S13–S16L, M). Control sense probes for *AfimGL3*, *AfimMYB5*, *AfimMYB6*, *AfimTRY* and *AfimTTG1* showed no signal (Fig. S12).

DISCUSSION

We provide a comprehensive analysis of trichome-related gene expression patterns in flowers of an early diverging angiosperm with a highly elaborate, trichome-dependent pollination system. Based on our expression data in *Aristolochia fimbriata*, floral trichomes use subset of core trichome development genes that appear to be deeply conserved, not only in sequence but also in expression patterns, across angiosperms. Altogether, the core trichome-related genes may control hooked trichome development in extra-floral organs such as the pedicel and the leaves of *Aristolochia fimbriata*. Thus, trichome formation inside the perianth may only require a group of genes including *AfimGL2*, *AfimHDG2*, *AfimMYB106*-like, *AfimRAV1-like* and *AfimWIN*.

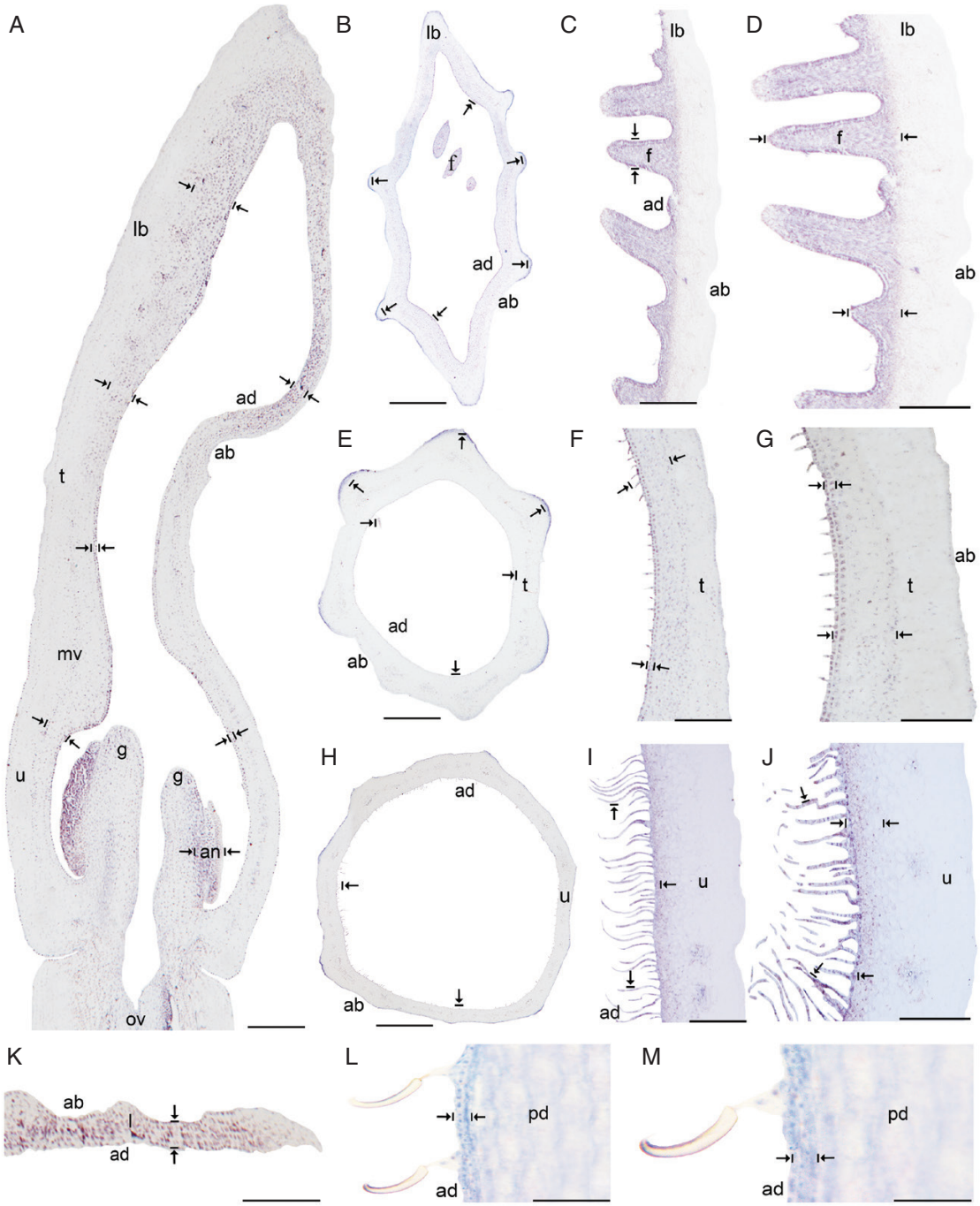

FIG. 6. *In situ* hybridization of *AfimRAV1*-like. (A) Sagittal section of the *Aristolochia fimbriata* flower at S6; note expression restricted to the adaxial mesophyll of the perianth. (B–D) Transverse (B) and longitudinal (C, D) sections of the limb at low (B), mid- (C) and high (D) magnification. (E–G) Transverse (E) and longitudinal (F, G) sections of the tube at low (E), mid- (F) and high (G) magnification. (H–J) Transverse (H) and longitudinal (I–J) sections of the utricle at low (H), mid- (I) and high (J) magnification. (K) Transverse section of the leaf. (L–M) Longitudinal section of the floral pedicel (L) and detail of its hooked trichomes (M). Arrow/bar signs point to detailed expression patterns; ab, abaxial epidermis; ad, adaxial epidermis; an, anther; fi, fimbriae; g, gynostemium; l, leaf; lb, limb; mv, midvein; ov, ovary; pd, pedicel; t, tube; u, utricle. Scale bars: 100 µm (A, B, E, H); 150 µm (C, F, I); 200 µm (D, G, J); 60 µm (K–M).

Expression of the remaining genes included in this study (*AfimGL3*, *AfimMYB5*, *AfimMYB6*, *AfimTRY* and *AfimTTG1*) show unexpected localization patterns, restricted to the abaxial and the adaxial perianth epidermis. Our results re-evaluate the core genetic network shaping trichome fate in flowers of early diverging angiosperms, resulting in a morphologically diverse output with a simpler genetic mechanism in place when compared to the model *Arabidopsis thaliana* and *Cucumis sativus*. In turn, it is likely that only the leaf trichome identity genetic regulatory network (GRN) is conserved across angiosperms.

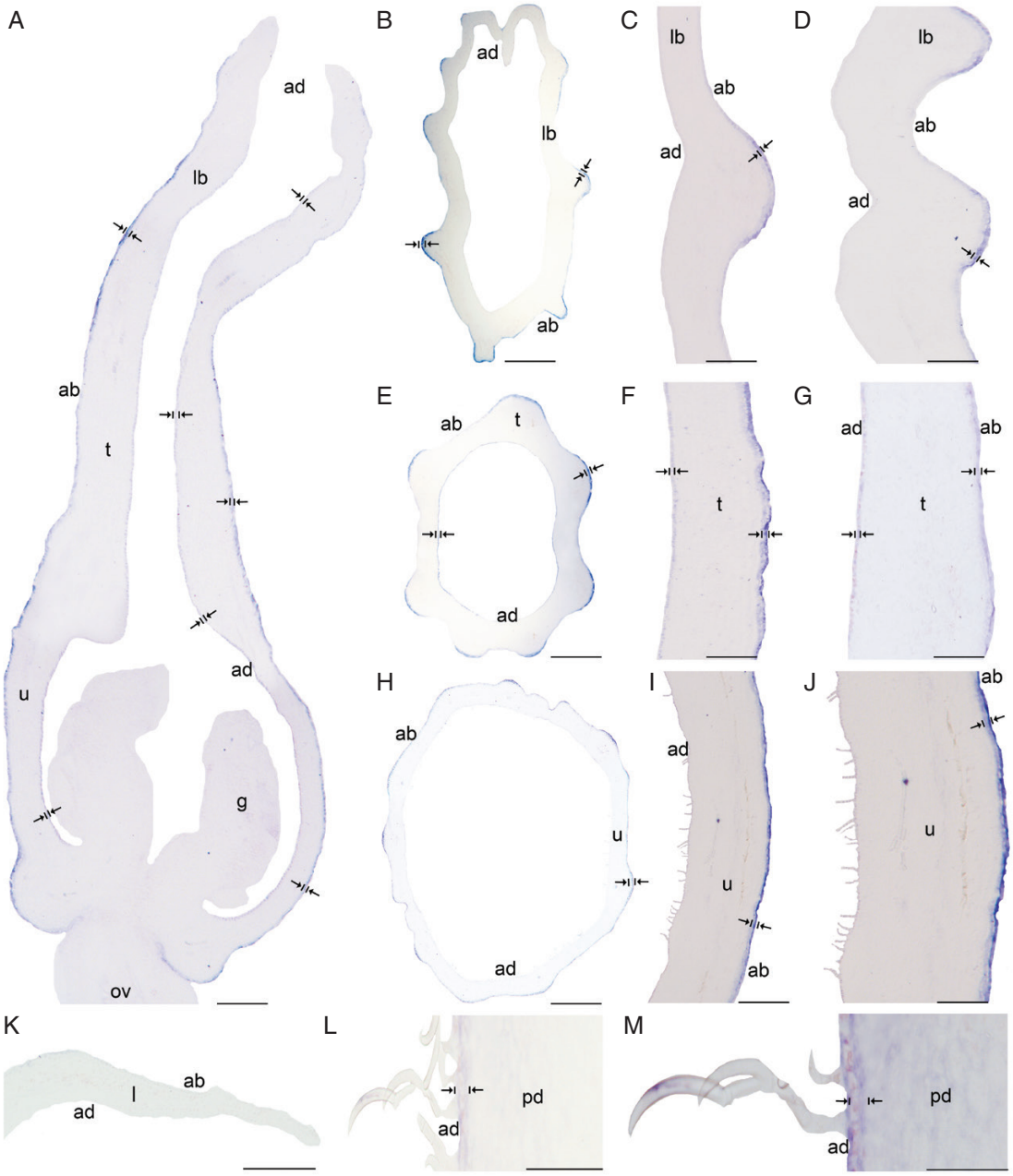

FIG. 7. *In situ* hybridization of *AfimHDG2*. (A) Sagittal section of the *Aristolochia fimbriata* flower at S6; note expression in the abaxial epidermis of the perianth, and weak expression in its adaxial counterpart. (B–D) Transverse (B) and longitudinal (C, D) sections of the limb at low (B), mid- (C) and high (D) magnification. (E–G) Transverse (E) and longitudinal (F, G) sections of the tube at low (E), mid- (F) and high (G) magnification. (H–J) Transverse (H) and longitudinal (I–J) sections of the utricle at low (H), mid- (I) and high (J) magnification. (K) Transverse section of the leaf. (L–M) Longitudinal section of the floral pedicel (L) and detail of its the hooked trichomes (M). Arrow/bar signs point to detailed expression patterns; ab, abaxial epidermis; ad, adaxial epidermis; fi, fimbriae; g, gynostemium; l, leaf; lb, limb; mv, midvein; ov, ovary; pd, pedicel; t, tube; u, utricle. Scale bars: 100 µm (A, B, E, H); 150 µm (C, F, I); 200 µm (D, G, J); 60 µm (K–M).

Few genes are common hubs for multicellular trichome development across distantly related angiosperm lineages

Aristolochia fimbriata, as a member of the magnoliid family Aristolochiaceae, whose ancestor pre-dates the diversification of monocots and eudicots, is particularly well positioned to assess floral trichome development genes recruited during early angiosperm evolution. Based on quantitative and qualitative expression patterns we showed that *AfimGL2*, *AfimMYB106*-like, *AfimRAV1*-like and *AfimWIN1* probably control the development of multicellular trichomes in the perianth of *Aristolochia fimbriata*. In addition, *AfimHDG2* may be involved in the differentiation of the inner and outer floral epidermis. Data available from other angiosperms confirm that these five TFs are common hubs for trichome development in stems, leaves and perianth. We discuss these TFs in order to identify the contribution of each gene lineage to trichome development in various angiosperms.

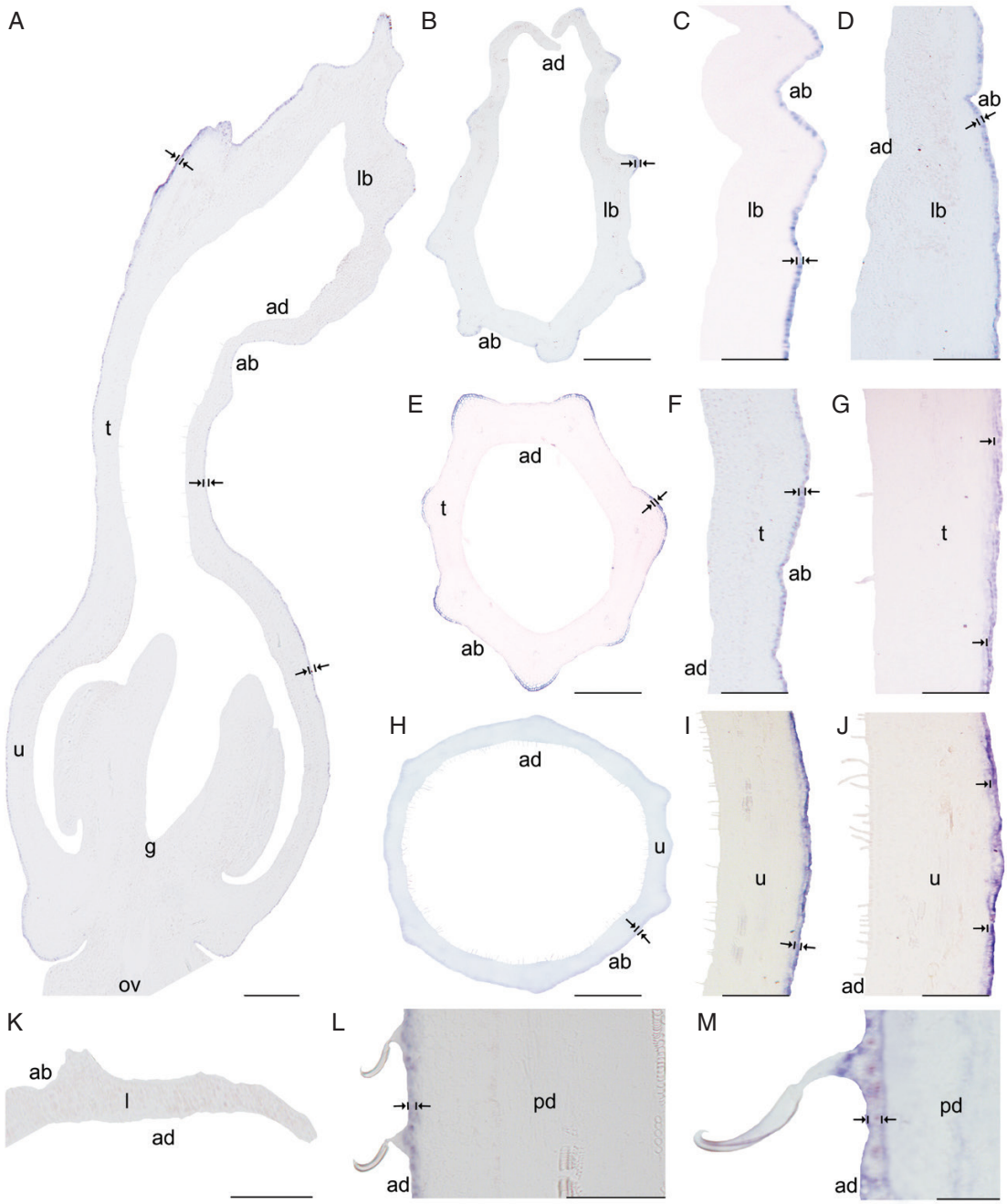

FIG. 8. *In situ* hybridization of *AfimTTG1*. (A) Sagittal section of the *Aristolochia fimbriata* flower at S6; note expression restricted to the abaxial epidermis of the perianth. (B–D) Transverse (B) and longitudinal (C, D) sections of the limb at low (B), mid- (C) and high (D) magnification. (E–G) Transverse (E) and longitudinal (F, G) sections of the tube at low (E), mid- (F) and high (G) magnification. (H–J) Transverse (H) and longitudinal (I, J) sections of the utricle at low (H), mid- (I) and high (J) magnification. (K) Transverse section of the leaf. (L and M) Longitudinal section of the floral pedicel (L) and detail of its hooked trichomes (M). Arrow/bar signs point to detailed expression patterns; ab, abaxial epidermis; ad, adaxial epidermis; fi, fimbriae; g, gynostemium; l, leaf; lb, limb; mv, midvein; ov, ovary; pd, pedicel; t, tube; u, utricle. Scale bars: 100 µm (A, B, E, H); 150 µm (C, F, I); 200 µm (D, G, J); 60 µm (K–M).

In *Aristolochia fimbriata*, the pattern of *AfimGL2* expression is maintained in the fimbriae and all trichome types distributed in the adaxial perianth epidermis (Fig. 3). These results suggest a fundamental role of *AfimGL2*, in both the initiation and the differentiation of multicellular trichomes. Similar processes have been attributed to *GL2* homologues in model eudicots with both unicellular and multicellular trichomes. In *Arabidopsis*, GLABRA2 (GL2) controls unicellular trichome initiation and branching as well as cell expansion and cell wall maturation (Koornneef *et al.*, 1982; Rerie *et al.*, 1994; Marks and Esch, 1994; Cristina *et al.*, 1996; Ohashi *et al.*, 2002). In *Cucumis sativus CsGL2* also controls multicellular trichome morphogenesis (Zhao *et al.*, 2015*b*; Liu *et al.*, 2016). The *csgl2* mutant exhibits few trichomes on the tendrils, sepals, ovaries

and fruits, and glabrous stems and leaves (Yang *et al.*, 2015). In turn, *GL2* homologues seem to be a key hub for trichome development across angiosperms, regardless of whether they are uni- or multicellular.

The *MYB106* homologues, best known as *MIXTA*-like R2R3 MYB genes, are pivotal conserved TFs in trichome development and epidermal specializations across angiosperms. Our study shows that *AfimMYB106*-like is expressed in the adaxial and the abaxial epidermis of the *Aristolochia fimbriata* perianth, including the secretory multicellular trichomes inside the tube and utricle (Fig. 4F, G, I, J). These expression patterns suggest that *AfimMYB106*-like plays a role in epidermal patterning and in multicellular development of both structural and secretory types of trichomes, similarly to homologues of other species. The *MYB106* homologue in Arabidopsis (*NOECK*) controls trichome branching (Folkers *et al.*, 1997; Stracke *et al.*, 2001; Jakoby *et al.*, 2008). *MIXTA*-like genes regulate the growth of epidermal conical cells in the *Antirrhinum majus* and *Nicotiana tabacum* petals (Noda *et al.*, 1994; Baumann *et al.*, 2007; Jaffé *et al.*, 2007). The *MYB106* homologue in cotton is *GhMYB25* and is expressed during the development of the long unicellular seed coat trichomes as well as trichomes in petals, stems and leaves (Wu *et al.*, 2006; Walford *et al.*, 2011; Machado *et al.*, 2009). Likewise, homologues of *AtMYB106* have been reported in *Cucumis sativus* as potential candidates for epidermal cell differentiation and trichome morphogenesis (Li *et al.*, 2012; Zhao *et al.*, 2015*b*; Yang *et al.*, 2018). Furthermore, in the non-core eudicot genus *Thalictrum* (Ranunculaceae), the orthologue of *MIXTA-like2* controls epidermal cell shape in flowers (Di Stilio *et al.*, 2009).

In comparison to the two TFs discussed before, *WIN1* and *RAV*-like homologues have been less studied. In turn, their association with trichome development across diverse angiosperm species is unclear. In *Aristolochia fimbriata*, *AfimWIN1* is continuously expressed in the adaxial and abaxial epidermis of the perianth and in all floral trichomes (Fig. 5). The *WIN1* homologue in *Arabidopsis* regulates the production of epicuticular waxes (Kannangara *et al.*, 2007). However, in *Cucumis sativus*, *CsWIN1* works as an essential regulator of multicellular trichome development, together with *CsGL2* and *CsMYB6* (Zhao *et al.*, 2015*a*; Liu *et al.*, 2016). Thus, it is possible that *WIN1* homologues were recruited early on during plant diversification in multicellular trichome development and unicellular trichomes do not actively need them.

It is also uncertain whether *RAV1-like* homologues are commonly recruited in trichome development across angiosperms. In *Aristolochia fimbriata*, *AfimRAV1*-like is continuously expressed in the adaxial pavement epidermal cells as well as the trichomes of the limb, tube, and utricle, which may suggest its positive role in multicellular trichome development (Fig. 6F-G, I-J). However, members of the *Arabidopsis RAV* family, such as *TEM1* and *TEM2*, repress trichome development by directing gibberellin accumulation and distribution in the leaf mesophyll (Matías-Hernández *et al.*, 2016), and regulating *GL1* and *GL2*. Conversely, a *RAV1*-like homolog has been suggested as a candidate gene in the development of multicellular trichomes in *Cucumis sativus* (Zhao *et al.*, 2015*a*). In turn, more information is needed across angiosperms to assess whether *RAV1*-like genes positively or negatively control uni- or multicellular trichome development.

Overall, our results regarding the expression patterns of *AfimGL2*, *AfimMYB106*-like, *AfimWIN1* and *AfimRAV1*-like genes in the perianth of *Aristolochia fimbriata* are consistent with those described above for model species such as *Cucumis sativus*, suggesting that these genes are players in the multicellular trichome genetic regulatory network. Our evidence indicates that the network in *Aristolochia fimbriata* is more similar to the GRN reported in cucumber. More comparative studies in non-model species will allow the identification of a common GRN for epidermal differentiation across angiosperms and the specific shifts in uni- versus multicellular trichome development.

Different GRNs control floral versus non-floral trichomes in Aristolochia fimbriata

Several genes have been identified as key TFs for unicellular and multicellular trichome development in *Arabidopsis thaliana* and *Cucumis sativus*, respectively. In *Arabidopsis* various trichome-related mutants have allowed the identification of trichome-positive and trichome-negative regulators (Fig. 2A). The positive regulators include *GLABROUS1* (*GL1*), which encodes an R2R3 MYB transcriptional regulator (Oppenheimer *et al.*, 1991) and a WD40 repeat-containing protein TRANSPARENT TESTA GLABRA1 (TTG1) (Bernhard *et al.*, 2005). Two additional positive regulators redundantly control trichome development; these are *GLABRA3* (*GL3*) and *ENHANCER OF GLABRA3* (*EGL3*), both bHLH-like TFs (Payne *et al.*, 2000; Balkunde *et al.*, 2011). These positive regulators stimulate trichome cell fate by activating the expression of *GLABRA2* (*GL2*), which encodes a homeodomain leucine-zipper (HD-Zip IV) (Rerie *et al.*, 1994). The trichome-negative regulators are represented by a set of single-repeat MYB proteins encoded by six redundant genes, namely *TRIPTYCHON* (*TRY*), *CAPRICE* (*CPC*), *ENHANCER OF TRY AND CPC1* (*ETC1*), *ETC2*, *ETC3* and *TRICHOMELESS1* (*TCL1*) (Schnittger *et al.*, 1999; Kirik *et al.*, 2004*a*, *b*; S. Wang *et al.*, 2007; Tominaga *et al.*, 2008; Y.L. Wang *et al.*, 2008; Yang and Ye, 2013). In addition to these negative regulators, *MYB5* has been reported to have a redundant role with the R2R3 MYB gene *TRANSPARENT TESTA GLABRA2* (*TTG2*), in the control of trichome development and tannin production (González *et al.*, 2009; Marks *et al.*, 2009). A slightly different positive regulatory network for multicellular trichome development has been proposed in *Cucumis sativus.* Positive trichome regulators include *TRIL*/*CsGL3*, which encodes a homeodomain leucine-zipper (HD-Zip) and its protein partner, an HD-Zip I protein. The complex putatively activates downstream genes triggering trichome development, including *CsMYB6*, *CsWIN1* and *CsGL2* (Chen *et al.*, 2014; Zhao *et al.*, 2015*a*, *b*; Liu *et al.*, 2016).

Using a candidate gene approach, we have identified and tested the expression patterns of *GL2*, *GL3*, *HDG2*, *MYB5*, *MYB6*, *MYB106*-like, *RAV1*-like, *TTG1*, *TRY* and *WIN1* homologues in *Aristolochia fimbriata.* All these genes might be controlling three-celled hooked trichome development in the floral pedicel, stem and leaves in this species (Figs 3–8K–M; Supplementary Data Figs S13–S16). In the hooked trichomes of the floral pedicel the

contribution of *AfimMYB5* and *AfimMYB6* stands out, as the two TFs are highly expressed in the apical, hooked-shaped cell (Figs S15, S16K–M). In *Arabidopsis*, *MYB5* has a redundant role regulating pleiotropic control of trichome development (González *et al*., 2009; Marks *et al.*, 2009). Likewise, *MYB6* has been reported as a candidate gene involved directly in multicellular trichome development (Zhao *et al*., 2015*a*, *b*). The *MYB6* homologue *CsMYB6* in *Cucumis sativus* positively regulates multicellular trichome development in stems, tendrils, leaves and flowers (Liu *et al.*, 2016), while it negatively regulates fruit trichome formation as part of the *CsMYB6-CsTRY* complex (Yang *et al.*, 2018). In *Aristolochia fimbriata MYB5* and *MYB6* are strongly expressed in the abaxial epidermis of the perianth and the pedicel epidermis. In turn, expression of the TFs *GL2*, *GL3*, *HDG2*, *MYB5*, *MYB6*, *MYB106*-like, *TRY*, *TTG1*, *RAV1*-like and *WIN1* in extra-floral trichomes suggests that they were already active in magnoliids, and their role later diverged in the core eudicots *Arabidopsis thaliana* and *Cucumis sativus*. Conversely, floral trichome fate in *Aristolochia fimbriata* relies on a smaller subset of genes that comprises *AfimGL2*, *AfimHDG2*, *AfimMYB106*-like, *AfimRAV1*-like and *AfimWIN1* (Figs 3–8).

Vascularized limb extensions (fimbriae) retain expression of AfimGL2, AfimMYB106-like, AfimRAV1-like and AfimWIN1

Our results show that genes controlling floral trichomes, such as *AfimGL2*, *AfimMYB106*-like, *AfimWIN1* and *AfimRAV1*-like, are also expressed in the marginal limb extensions, known as the fimbriae (Figs 1B, F, 3, 5 and 6C, D). The fimbriae are multicellular, vascularized outgrowths with epidermal osmophores and hooked trichomes (Pabón-Mora *et al.*, 2015). The fimbriae probably act as the first visual and olfactory signals to pollinators in *Aristolochia fimbriata* (Aliscioni *et al.*, 2017). Expression of *AfimGL2*, *AfimMYB106*-like, *AfimRAV1*-like and *AfimWIN1* is detected throughout the fimbria epidermis and vascular tissue, and also in the three to six subepidermal cell layers (Figs 3, 4C, D, 5 and 6C, D). Different homeobox-leucine zipper genes that encode proteins such as GL2 and ANTHOCYANINLESS2 (ANL2) have been reported in transcriptional networks involved in cell differentiation and anthocyanin pigmentation, not only in the epidermis but also in the leaf subepidermal tissue layers (Kubo *et al.*, 1999; Qing and Aoyama, 2012). In addition, members of the *RAV* family such as the *TEMPRANILLO* (*TEM1* and *TEM2*) genes, also play an essential role in controlling trichome initiation at the epidermal and subepidermal levels (Matías-Hernández *et al.*, 2016). Together, these results point to common GRNs for the limb fimbriae, the adaxial epidermis of the tube and the utricle, and floral trichome initiation and differentiation in *Aristolochia fimbriata.*

The abaxial perianth epidermis retains expression of a subset of TFs

In *Aristolochia fimbriata*, *AfimTTG1*, *AfimGL3* and *AfimTRY* showed expression patterns restricted to the abaxial glabrous epidermis of the perianth in the limb (Fig. 8A–D; Supplementary Data Figs S13 and S14A–D), tube (Fig. 8E–G; Figs S13 and S14E, G) and utricle (Fig. 8H–J; Figs S13 and S14H–J). Thus, our results suggest that although these TFs are signalling in the epidermal layers, they do not contribute directly to the formation of floral trichomes in *Aristolochia fimbriata.* The TFs *AfimGL3*, *AfimTRY* and *AfimTTG1* are homologues to those of the *Arabidopsis* genetic regulatory network that drive unicellular trichome development. *TTG1* is the common denominator of overlapping regulatory complexes that control cell fate and trichome differentiation (Galway *et al.*, 1994; Walker *et al.*, 1999). *GL3* encodes an activator of trichome development (Hülskamp *et al.*, 1994; Koornneef *et al.*, 1982). Finally, *TRY* was the first negative regulator of trichome development identified (Hülskamp *et al.*, 1994; Balkunde *et al.*, 2011). The *try* mutants have trichomes occasionally arranged in clusters of two or three, suggesting that *TRY* represses trichome initiation in the neighbouring pavement epidermal cells (Schellmann *et al.*, 2002). In particular, expression of *AfimTRY* in the abaxial epidermis might be associated with the lack of trichomes in this layer of the perianth, probably functioning as a repressor of the genetic pathway. In turn, our results show that specialization and elaboration between the adaxial and the abaxial perianth epidermis relies on different sets of TFs, where repressive TFs become restricted to the non-specialized and highly homogeneous abaxial perianth surface. Thus, the *Aristolochia* perianth becomes paradoxical as the extremely elaborate adaxial epidermis and its structural and secretory trichomes require fewer trichome-related genes than its abaxial counterpart.

SUPPLEMENTARY DATA

Supplementary data are available online at https://academic.oup.com/aob and consist of the following. Figure S1. ML phylogenetic analysis of the *GL2* gene lineage in flowering plants. Figure S2. ML phylogenetic analysis of the *GL3* gene lineage in flowering plants. Figure S3. ML phylogenetic analysis of the *TTG1* gene lineage in flowering plants. Figure S4. ML phylogenetic analysis of the *TRY* gene lineage in flowering plants. Figure S5. ML phylogenetic analysis of the *RAV1*-like gene lineage in flowering plants. Figure S6. ML phylogenetic analysis of the *MYB5* gene lineage in flowering plants. Figure S7. ML phylogenetic analysis of the *MYB6* gene lineage in flowering plants. Figure S8. ML phylogenetic analysis of the *MYB106*-like gene lineage in flowering plants. Figure S9. ML phylogenetic analysis of the *WIN1* gene lineage in flowering plants. Figure S10. ML phylogenetic analysis of the *HDG2* gene lineage in flowering plants. Figure S11. *In situ* hybridization of *AfimGL2*, *AfimGL3*, *AfimTTG1*, *AfimTRY*, *AfimRAV1*-like, *AfimMYB5*, *AfimMYB6*, *AfimHDG2*-like, *AfimMYB106*-like *and AfimWIN1* at the flowering shoot apex. Figure S12. *In situ* sense probes used as controls for the *Aristolochia fimbriata* epidermal flower candidate genes. Figure S13. *In situ* hybridization of *AfimGL3.* Figure S14. *In situ* hybridization of *AfimTRY.* Figure S15. *In situ* hybridization of *AfimMYB5.* Figure S16. *In situ* hybridization of *AfimMYB6.* Table S1. *De novo* assembly statistics of the floral transcriptomes of *Aristolochia fimbriata* at two different developmental stages. Table S2. Accession numbers of *GL2*, *GL3*, *HDG2*-like, *MIXTA*-like, *MYB5*, *MYB6*, *RAV1*-like, *TTG1*, *TRY* and *WIN1* homologue sequences used in this study. Table S3. Expression of the candidate genes included in this study. Table S4. Specific primers used in this study for the *in situ* hybridization experiments, including *AfimGL2*, *AfimGL3*, *AfimHDG2*, *AfimMYB5*,

AfimMYB6, *AfimMYB106*-like, *AfimRAV1*-like, *AfimTRY*, *AfimTTG1* and *AfimWIN1* orthologues in *Aristolochia fimbriata.*

ACKNOWLEDGEMENTS

We especially thank the Arnold Arboretum at Harvard University and the New York Botanical Garden (NYBG) for their support during this research. We also thank Cecilia Zumajo-Cardona (NYBG) for assistance during lab work. N.P.-M., F.G., S.P., B.A. and H.S.-B. conceived and designed the study; N.P.-M. and H.S.-B. performed the experiments, and acquired, analysed and interpreted the data; J.F.A., N.P.-M. and H.S.-B. executed the bioinformatics analysis and analysed data; H.S.-B., F.G. and N.P.-M. wrote the manuscript, and all authors revised and approved the final manuscript.

FUNDING

This work was supported by COLCIENCIAS/COLFUTURO (Conv. Doctorados Nacionales No. 727 de 2015), the Deland Award, 2018 to H.S.-B. (the Arnold Arboretum at Harvard University), and Estrategia de Sostenibilidad (2018–2019) awarded to the Grupo Evo-Devo en Plantas by the Universidad de Antioquia, Medellín, Colombia.

LITERATURE CITED

Aliscioni SS, Achler AP, Torretta JP. 2017. Floral anatomy, micromorphology and visitor insects in three species of *Aristolochia* L. (Aristolochiaceae). *New Zealand Journal of Botany* **55**: 496–513.

Ambrose BA, Lerner DR, Ciceri P, Padilla CM, Yanofsky MF, Schmidt RJ. 2000. Molecular and genetic analyses of the *Silky1* gene reveal conservation in floral organ specification between eudicots and monocots. *Molecular Cell* **5**: 569–579.

Balkunde R, Pesch M, Hülskamp M. 2011. Trichome patterning in *Arabidopsis thaliana*: from genetic to molecular models. *Current Topics in Developmental Biology* **91**: 299–321.

Baumann K, Perez-Rodriguez M, Bradley D, *et al.* 2007. Control of cell and petal morphogenesis by *R2R3 MYB* transcription factors. *Development (Cambridge, England)* **134**: 1691–1701.

Bernhardt C, Lee MM, Gonzalez A, Zhang F, Lloyd A, Schiefelbein J. 2003. The bHLH genes *GLABRA3* (*GL3*) and *ENHANCER OF GLABRA3* (*EGL3*) specify epidermal cell fate in the Arabidopsis root. *Development (Cambridge, England)* **130**: 6431–6439.

Bernhardt C, Zhao M, Gonzalez A, Lloyd A, Schiefelbein J. 2005. The bHLH genes *GL3* and *EGL3* participate in an intercellular regulatory circuit that controls cell patterning in the *Arabidopsis* root epidermis. *Development (Cambridge, England)* **132**: 291–298.

Boff S, Demarco D, Marchi P, Alves-Dos-Santos I. 2015. Perfume production in flowers of *Angelonia salicariifolia* attracts males of *Euglossa annectans* which do not promote pollination. *Apidologie* **46**: 84–91.

Bray NL, Pimentel H, Melsted P, Pachter L. 2016. Near-optimal probabilistic RNA-seq quantification. *Nature Biotechnology* **34**: 525–527.

Chen C, Liu M, Jiang L, *et al.* 2014. Transcriptome profiling reveals roles of meristem regulators and polarity genes during fruit trichome development in cucumber (*Cucumis sativus* L.). *Journal of Experimental Botany* **65**: 4943–4958.

Cocucci AA. 1991. Pollination biology of *Nierembergia* (Solanaceae). *Plant Systematics and Evolution* **174**: 17–35.

Cropper SC, Calder DM. 1990. The floral biology of *Thelymitra epipactoides* (*Orchidaceae*), and the implications of pollination by deceit on the survival of this rare orchid. *Plant Systematics and Evolution* **170**: 11–27.

Cui JY, Miao H, Ding LH, *et al.* 2016. A new glabrous gene (*csgl3*) identified in trichome development in cucumber (*Cucumis sativus* L.). *PLoS One* **11**: e0148422.

Dafni A. 1984. Mimicry and deception in pollination. *Annual Review of Ecology, Evolution, and Systematics* **15**: 259–278.

Di Cristina M, Sessa G, Dolan L, *et al.* 1996. The *Arabidopsis* Athb-10 (GLABRA2) is an HD-Zip protein required for regulation of root hair development. *The Plant Journal: for Cell and Molecular Biology* **10**: 393–402.

Di Stilio VS, Martin C, Schulfer AF, Connelly CF. 2009. An ortholog of *MIXTA-like2* controls epidermal cell shape in flowers of *Thalictrum*. *The New Phytologist* **183**: 718–728.

Digiuni S, Schellmann S, Geier F, *et al.* 2008. A competitive complex formation mechanism underlies trichome patterning on Arabidopsis leaves. *Molecular Systems Biology* **4**: 217.

El Ottra JH, Pirani JR, Endress PK. 2013. Fusion within and between whorls of floral organs in Galipeinae (Rutaceae): structural features and evolutionary implications. *Annals of Botany* **111**: 821–837.

Erbar C, Heiler A, Leins P. 2016. Nectaries in fly-deceptive pitcher-trap blossoms of *Aristolochia*. *Flora* **232**: 128–141.

Esch JJ, Chen MA, Hillestad M, Marks MD. 2004. Comparison of *TRY* and the closely related *At1g01380* gene in controlling *Arabidopsis* trichome patterning. *The Plant Journal: for Cell and Molecular Biology* **40**: 860–869.

Ferrándiz C, Gu Q, Martienssen R, Yanofsky MF. 2000. Redundant regulation of meristem identity and plant architecture by *FRUITFULL*, *APETALA1* and *CAULIFLOWER*. *Development (Cambridge, England)* **127**: 725–734.

Folkers U, Berger J, Hülskamp M. 1997. Cell morphogenesis of trichomes in *Arabidopsis*: differential control of primary and secondary branching by branch initiation regulators and cell growth. *Development (Cambridge, England)* **124**: 3779–3786.

Galway ME, Masucci JD, Lloyd AM, Walbot V, Davis RW, Schiefelbein JW. 1994. The *TTG* gene is required to specify epidermal cell fate and cell patterning in the *Arabidopsis* root. *Developmental Biology* **166**: 740–754.

Glover BJ. 2000. Differentiation in plant epidermal cells. *Journal of Experimental Botany* **51**: 497–505.

Glover BJ, Perez-Rodriguez M, Martin C. 1998. Development of several epidermal cell types can be specified by the same MYB-related plant transcription factor. *Development (Cambridge, England)* **125**: 3497–3508.

Gonzalez A, Mendenhall J, Huo Y, Lloyd A. 2009. TTG1 complex MYBs, MYB5 and TT2, control outer seed coat differentiation. *Developmental Biology* **325**: 412–421.

González F, Pabón-Mora N. 2015. Trickery flowers: the extraordinary chemical mimicry of *Aristolochia* to accomplish deception to its pollinators. *New Phytologist* **206**: 10–13.

González F, Stevenson DW. 2000. Perianth development and systematics of *Aristolochia*. *Flora* **195**: 370–391.

Hu S, Dilcher DL, Jarzen DM, Taylor DW. 2008. Early steps of angiosperm–pollinator coevolution. *Proceedings of the National Academy of Sciences USA* **105**: 240–245.

Hülskamp M. 2004. Plant trichomes: a model for cell differentiation. *Nature Reviews Molecular Cell Biology* **5**: 471–480.

Hülskamp M, Miséra S, Jürgens G. 1994. Genetic dissection of trichome cell development in *Arabidopsis*. *Cell* **76**: 555–566.

Ioannidi E, Rigas S, Tsitsekian D, *et al.* 2016. Trichome patterning control involves TTG1 interaction with SPL transcription factors. *Plant Molecular Biology* **92**: 675–687.

Jaffé FW, Tattersall A, Glover BJ. 2007. A truncated MYB transcription factor from *Antirrhinum majus* regulates epidermal cell outgrowth. *Journal of Experimental Botany* **58**: 1515–1524.

Jakoby MJ, Falkenhan D, Mader MT, *et al.* 2008. Transcriptional profiling of mature Arabidopsis trichomes reveals that *NOECK* encodes the MIXTA-like transcriptional regulator MYB106. *Plant Physiology* **148**: 1583–1602.

Javelle M, Vernoud V, Rogowsky PM, Ingram GC. 2011. Epidermis: the formation and functions of a fundamental plant tissue. *The New Phytologist* **189**: 17–39.

Kannangara R, Branigan C, Liu Y, *et al.* 2007. The transcription factor WIN1/SHN1 regulates cutin biosynthesis in *Arabidopsis thaliana*. *The Plant Cell* **19**: 1278–1294.

Karabourniotis G, Papadopoulos K, Papamarkou M, Manetas Y. 1992. Ultraviolet-B radiation absorbing capacity of leaf hairs. *Physiologia Plantarum* **86**: 414–418.

Kärkkäinen K, Agren J. 2002. Genetic basis of trichome production in *Arabidopsis lyrata*. *Hereditas* **136**: 219–226.

Katoh K, Misawa K, Kuma K, Miyata T. 2002. MAFFT: a novel method for rapid multiple sequence alignment based on fast Fourier transform. *Nucleic Acids Research* **30**: 3059–3066.

Kirik V, Lee MM, Wester K, *et al.* 2005. Functional diversification of *MYB23* and *GL1* genes in trichome morphogenesis and initiation. *Development (Cambridge, England)* **132**: 1477–1485.

Kirik V, Simon M, Huelskamp M, Schiefelbein J. 2004*a*. The *ENHANCER OF TRY AND CPC1* gene acts redundantly with *TRIPTYCHON* and *CAPRICE* in trichome and root hair cell patterning in *Arabidopsis*. *Developmental Biology* **268**: 506–513.

Kirik V, Simon M, Wester K, Schiefelbein J, Hulskamp M. 2004*b*. *ENHANCER* of *TRY* and *CPC2* (*ETC2*) reveals redundancy in the region-specific control of trichome development of Arabidopsis. *Plant Molecular Biology* **55**: 389–398.

Koornneef M, Dellaert LW, van der Veen JH. 1982. EMS- and radiation-induced mutation frequencies at individual loci in *Arabidopsis thaliana* (L.) Heynh. *Mutation Research* **93**: 109–123.

Kubo H, Peeters AJ, Aarts MG, Pereira A, Koornneef M. 1999. *ANTHOCYANINLESS2*, a homeobox gene affecting anthocyanin distribution and root development in Arabidopsis. *The Plant Cell* **11**: 1217–1226.

Larkin JC, Marks MD, Nadeau J, Sack F. 1997. Epidermal cell fate and patterning in leaves. *The Plant Cell* **9**: 1109–1120.

Larkin JC, Young N, Prigge M, Marks MD. 1996. The control of trichome spacing and number in *Arabidopsis*. *Development (Cambridge, England)* **122**: 997–1005.

Levin DA. 1973. The role of trichomes in plant defense. *The Quarterly Review of Biology* **48**: 3–15.

Li Q, Cao C, Zhang C, *et al.* 2015. The identification of *Cucumis sativus Glabrous1 (CsGL1)* required for the formation of trichomes uncovers a novel function for the homeodomain-leucine zipper I gene. *Journal of Experimental Botany* **66**: 2515–2526.

Li Q, Zhang C, Li J, Wang L, Ren Z. 2012. Genome-wide identification and characterization of R2R3MYB family in *Cucumis sativus*. *PLoS One* **7**: e47576.

Li SF, Milliken ON, Pham H, *et al.* 2009. The *Arabidopsis* MYB5 transcription factor regulates mucilage synthesis, seed coat development, and trichome morphogenesis. *The Plant Cell* **21**: 72–89.

Liu S, Jiao J, Lu TJ, Xu F, Pickard BG, Genin GM. 2017. *Arabidopsis* leaf trichomes as acoustic antennae. *Biophysical Journal* **113**: 2068–2076.

Liu X, Bartholomew E, Cai Y, Ren H. 2016. Trichome-related mutants provide a new perspective on multicellular trichome initiation and development in cucumber (*Cucumis sativus* L). *Frontiers in Plant Science* **7**: 1187.

Machado A, Wu Y, Yang Y, Llewellyn DJ, Dennis ES. 2009. The MYB transcription factor *GhMYB25* regulates early fibre and trichome development. *The Plant Journal: for Cell and Molecular Biology* **59**: 52–62.

Marks MD, Esch JJ. 1994. Morphology and development of mutant and wild type trichomes on the leaves of *Arabidopsis thaliana*. In: Bowman J, ed. *Arabidopis: An atlas of morphology and development*. New York: Springer, 56–73.

Marks MD, Wenger JP, Gilding E, Jilk R, Dixon RA. 2009. Transcriptome analysis of *Arabidopsis* wild-type and *gl3*-sst sim trichomes identifies four additional genes required for trichome development. *Molecular Plant* **2**: 803–822.

Martins AC, Aguiar AJC, Alves-Dos-Santos I. 2013. Interaction between oil-collecting bees and seven species of Plantaginaceae. *Flora* **208**: 401–411.

Masucci JD, Rerie WG, Foreman DR, *et al.* 1996. The homeobox gene *GLABRA2* is required for position-dependent cell differentiation in the root epidermis of *Arabidopsis thaliana*. *Development (Cambridge, England)* **122**: 1253–1260.

Matías-Hernández L, Aguilar-Jaramillo AE, Osnato M, *et al.* 2016. TEMPRANILLO reveals the mesophyll as crucial for epidermal trichome Formation. *Plant Physiology* **170**: 1624–1639.

Miller M, Pfeiffer W, Schwartz T. 2010. Creating the CIPRES science gateway for inference of large phylogenetic trees. Gateway Computing Environments Workshop (GCE) 1-8.

Netolitzky F. 1932. *Die Pflanzenhaare. Handbuch der Pflanzenanatomie.* Berlin: Gebrüder Borntraeger.

Noda K, Glover BJ, Linstead P, Martin C. 1994. Flower colour intensity depends on specialized cell shape controlled by a Myb-related transcription factor. *Nature* **369**: 661–664.

Oelschlägel B, Gorb S, Wanke S, Neinhuis C. 2009. Structure and biomechanics of trapping flower trichomes and their role in the pollination biology of *Aristolochia* plants (Aristolochiaceae). *The New Phytologist* **184**: 988–1002.

Ohashi Y, Oka A, Ruberti I, Morelli G, Aoyama T. 2002. Entopically additive expression of GLABRA2 alters the frequency and spacing of trichome initiation. *The Plant Journal* **21**: 5036–5046.

Oppenheimer DG, Herman PL, Sivakumaran S, Esch J, Marks MD. 1991. A myb gene required for leaf trichome differentiation in *Arabidopsis* is expressed in stipules. *Cell* **67**: 483–493.

Pabón-Mora N, Suárez-Baron H, Ambrose BA, González F. 2015. Flower development and perianth identity candidate genes in the basal angiosperm *Aristolochia fimbriata* (Piperales: Aristolochiaceae). *Frontiers in Plant Science* **6**: 1095.

Pan Y, Bo K, Cheng Z, Weng Y. 2015. The loss-of-function *GLABROUS3* mutation in cucumber is due to LTR-retrotransposon insertion in a class IV HD-ZIP transcription factor gene *CsGL3* that is epistatic over *CsGL1*. *BMC Plant Biology* **15**: 302.

Pattanaik S, Patra B, Singh SK, Yuan L. 2014. An overview of the gene regulatory network controlling trichome development in the model plant, *Arabidopsis*. *Frontiers in Plant Science* **5**: 259.

Payne CT, Zhang F, Lloyd AM. 2000. GL3 encodes a bHLH protein that regulates trichome development in arabidopsis through interaction with GL1 and TTG1. *Genetics* **156**: 1349–1362.

Payne T, Clement J, Arnold D, Lloyd A. 1999. Heterologous myb genes distinct from GL1 enhance trichome production when overexpressed in *Nicotiana tabacum*. *Development (Cambridge, England)* **126**: 671–682.

Pérez-Rodríguez M, Jaffé FW, Butelli E, Glover BJ, Martin C. 2005. Development of three different cell types is associated with the activity of a specific MYB transcription factor in the ventral petal of *Antirrhinum majus* flowers. *Development* **132**: 359–370.

Pesch M, Hülskamp M. 2004. Creating a two-dimensional pattern *de novo* during *Arabidopsis* trichome and root hair initiation. *Current Opinion in Genetics & Development* **14**: 422–427.

Pesch M, Hülskamp M. 2009. One, two, three.models for trichome patterning in Arabidopsis? *Current Opinion in Plant Biology* **12**: 587–592.

Peterson KM, Shyu C, Burr CA, *et al.* 2013. *Arabidopsis* homeodomain-leucine zipper IV proteins promote stomatal development and ectopically induce stomata beyond the epidermis. *Development (Cambridge, England)* **140**: 1924–1935.

Płachno BJ, Stpiczńska M, Adamec L, Oliveira-Miranda VF, Świątek P. 2018. Nectar trichome structure of aquatic bladderworts from the section *Utricularia* (Lentibulariaceae) with observation of flower visitor and pollinators. *Protoplasma* **255**: 1053–1064.

Płachno BJ, Stpiczńska M, Świątek P, *et al.* 2019. Floral micromorphology and nectar composition of the early evolutionary lineage *Utricularia* (subgenus *Polypompholyx*, Lentibulariaceae). *Protoplasma* **256**: 1531–1543.

Qing L, Aoyama T. 2012. Pathways for epidermal cell differentiation via the homeobox gene *GLABRA*2: update on the roles of the classic regulator. *Journal of Integrative Plant Biology* **54**: 729–737.

Rambaut A. 2014. *FigTree: Tree Figure Drawing Tool, version 1.4.4*. Institute of Evolutionary Biology, University of Edinburgh. http://tree.bio.ed.ac.uk/software/figtree/ (1 December 2019).

Rerie WG, Feldmann KA, Marks MD. 1994. The *GLABRA2* gene encodes a homeodomain protein required for normal trichome development in *Arabidopsis*. *Genes and Development* **8**: 1388–1399.

Schellmann S, Schnittger A, Kirik V, *et al.* 2002. *TRIPTYCHON* and *CAPRICE* mediate lateral inhibition during trichome and root hair patterning in *Arabidopsis*. *The EMBO Journal* **21**: 5036–5046.

Schiefelbein J. 2003. Cell-fate specification in the epidermis: a common patterning mechanism in the root and shoot. *Current Opinion in Plant Biology* **6**: 74–78.

Schnittger A, Folkers U, Schwab B, Jürgens G, Hülskamp M. 1999. Generation of a spacing pattern: the role of *TRIPTYCHON* in trichome patterning in Arabidopsis. *The Plant Cell* **11**: 1105–1116.

Schnittger A, Hülskamp M. 2002. Trichome morphogenesis: a cell-cycle perspective. *Philosophical Transactions of the Royal Society of London. Series B, Biological Sciences* **357**: 823–826.

Schwab B, Folkers U, Ilgenfritz H, Hülskamp M. 2000. Trichome morphogenesis in *Arabidopsis*. *Philosophical Transactions of the Royal Society of London. Series B, Biological Sciences* **355**: 879–883.

Serna L, Martin C. 2006. Trichome: different regulatory network lead to convergent structures. *Trends in Plant Science* **11**: 1360–1385.

Simon M, Bruex A, Kainkaryam RM, *et al.* 2013. Tissue-specific profiling reveals transcriptome alterations in *Arabidopsis* mutants lacking morphological phenotypes. *The Plant Cell* **25**: 3175–3185.

Stamatakis A, Hoover P, Rougemont J. 2008. A rapid bootstrap algorithm for the RAxML Web servers. *Systematic Biology* **57**: 758–771.

Stpiczyńska M, Kamińska M, Davies KL, Pansarin ER. 2018. Nectar-secreting and nectarless *Epidendrum*: structure of the inner floral spur. *Frontiers in Plant Science* **9**: 840.

Stracke R, Werber M, Weisshaar B. 2001. The R2R3-MYB gene family in *Arabidopsis thaliana*. *Current Opinion in Plant Biology* **4**: 447–456.

Suárez-Baron H, Alzate JF, González F, Ambrose BA, Pabón-Mora N. 2019. Genetic mechanisms underlying perianth epidermal elaboration of *Aristolochia ringens* Vahl (Aristolochiaceae). *Flora* **253**: 56–66.

Szymanski DB, Lloyd AM, Marks MD. 2000. Progress in the molecular genetic analysis of trichome initiation and morphogenesis in *Arabidopsis*. *Trends in Plant Science* **5**: 214–219.

Szymanski DB, Marks MD. 1998. *GLABROUS1* overexpression and *TRIPTYCHON* alter the cell cycle and trichome cell fate in *Arabidopsis*. *The Plant Cell* **10**: 2047–2062.

Tan J, Walford SA, Dennis ES, Llewellyn D. 2016. Trichomes control flower bud shape by linking together young petals. *Nature Plants* **2**: 16093.

Tominaga R, Iwata M, Sano R, Inoue K, Okada K, Wada T. 2008. *Arabidopsis CAPRICE-LIKE MYB 3 (CPL3)* controls endoreduplication and flowering development in addition to trichome and root hair formation. *Development (Cambridge, England)* **135**: 1335–1345.

Wada T, Kurata T, Tominaga R, *et al.* 2002. Role of a positive regulator of root hair development, *CAPRICE*, in Arabidopsis root epidermal cell differentiation. *Development (Cambridge, England)* **129**: 5409–5419.

Wada T, Tachibana T, Shimura Y, Okada K. 1997. Epidermal cell differentiation in *Arabidopsis* determined by a *Myb* homolog, CPC. *Science (New York, N.Y.)* **277**: 1113–1116.

Wagner GJ. 1991. Secreting glandular trichomes: more than just hairs. *Plant Physiology* **96**: 675–679.

Wagner GJ, Wang E, Shepherd RW. 2004. New approaches for studying and exploiting an old protuberance, the plant trichome. *Annals of Botany* **93**: 3–11.

Walford SA, Wu Y, Llewellyn DJ, Dennis ES. 2011. GhMYB25-like: a key factor in early cotton fibre development. *The Plant Journal: for Cell and Molecular Biology* **65**: 785–797.

Walker AR, Davison PA, Bolognesi-Winfield AC, *et al.* 1999. The TRANSPARENT TESTA GLABRA1 locus, which regulates trichome differentiation and anthocyanin biosynthesis in Arabidopsis, encodes a WD40 repeat protein. *The Plant Cell* **11**: 1337–1350.

Wang S, Hubbard L, Chang Y, Guo J, Schiefelbein J, Chen JG. 2008. Comprehensive analysis of single-repeat R3 MYB proteins in epidermal cell patterning and their transcriptional regulation in *Arabidopsis*. *BMC Plant Biology* **8**: 81.

Wang S, Kwak SH, Zeng Q, *et al.* 2007. *TRICHOMELESS1* regulates trichome patterning by suppressing *GLABRA1* in Arabidopsis. *Development (Cambridge, England)* **134**: 3873–3882.

Wang YL, Nie JT, Chen HM, *et al.* 2016. Identification and mapping of *Tril*, a homeodomain-leucine zipper gene involved in multicellular trichome initiation in *Cucumis sativus*. *TAG. Theoretical and Applied Genetics. Theoretische und Angewandte Genetik* **129**: 305–316.

Werker E. 2000. Trichome diversity and development. *Advances in Botanical Research* **31**: 1–35.

Wu Y, Machado AC, White RG, Llewellyn DJ, Dennis ES. 2006. Expression profiling identifies genes expressed early during lint fibre initiation in cotton. *Plant & Cell Physiology* **47**: 107–127.

Yang C, Gao Y, Gao S, *et al.* 2015. Transcriptome profile analysis of cell proliferation molecular processes during multicellular trichome formation induced by tomato *Wov* gene in tobacco. *BMC Genomics* **16**: 868.

Yang C, Ye Z. 2013. Trichomes as models for studying plant cell differentiation. *Cellular and Molecular Life Sciences: CMLS* **70**: 1937–1948.

Yang S, Cai Y, Liu X, *et al.* 2018. A *CsMYB6-CsTRY* module regulates fruit trichome initiation in cucumber. *Journal of Experimental Botany* **69**: 1887–1902.

Young AM, Schaller M, Strand M. 1984. Floral nectaries and trichomes in relation to pollination in some species of *Theobroma* and *Herrania* (Sterculiaceae). *American Journal of Botany* **71**: 466–480.

Zhang F, Gonzalez A, Zhao M, Payne CT, Lloyd A. 2003. A network of redundant bHLH proteins functions in all TTG1-dependent pathways of *Arabidopsis*. *Development (Cambridge, England)* **130**: 4859–4869.

Zhao JL, Pan JS, Guan Y, *et al.* 2015*a*. Transcriptome analysis in *Cucumis sativus* identifies genes involved in multicellular trichome development. *Genomics* **105**: 296–303.

Zhao JL, Pan JS, Guan Y, *et al.* 2015*b*. Micro-trichome as a class I homeodomain-leucine zipper gene regulates multicellular trichome development in *Cucumis sativus*. *Journal of Integrative Plant Biology* **57**: 925–935.

Zhao M, Morohashi K, Hatlestad G, Grotewold E, Lloyd A. 2008. The TTG1-bHLH-MYB complex controls trichome cell fate and patterning through direct targeting of regulatory loci. *Development (Cambridge, England)* **135**: 1991–1999.

Zhou LH, Liu SB, Wang PF, *et al.* 2016. The *Arabidopsis* trichome is an active mechanosensory switch. *Plant, Cell & Environment* **40**: 611–621.